CRITICAL EVALUATION OF THE CORRELATIONS USED FOR ESTIMATING GEOMECHANICAL PROPERTIES FOR THE NIGER DELTA

A thesis presented to the Department of Petroleum Engineering,

African University of Science and Technology

In partial fulfilment of the requirements

for the degree of

MASTER OF SCIENCE

By

UZOCHUKWU MARYANN IFEOMA

Supervised by

Professor David O. Ogbe

African University of Science and Technology
www.aust.edu.ng
P.M.B 681, Garki, Abuja F.C.T
Nigeria

June, 2016

CRITICAL EVALUATION OF THE CORRELATIONS USED FOR ESTIMATING GEOMECHANICAL PROPERTIES FOR THE NIGER DELTA

By

Uzochukwu Maryann Ifeoma

A THESIS APPROVED BY THE PETROLEUM ENGINEERING DEPARTMENT

RECOMMENDED: ……..

Supervisor, Professor David O. Ogbe

……

Committee Member, Professor Djebbar Tiab

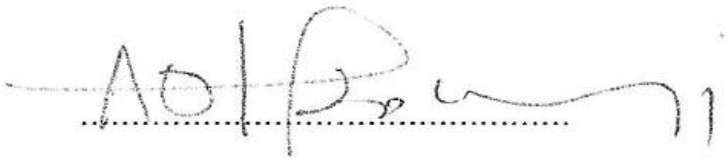

Committee Member, Dr. Alpheus Igbokoyi

……

Head, Department of Petroleum Engineering

APPROVED BY: ……..

Chief Academic Officer

.....

Date

ABSTRACT

The study area which is the Niger Delta Province is predominantly an unconsolidated sandstone terrain, the sand grains are friable suggesting the expectation of some geomechanical problems while developing hydrocarbon reserves in such terrain. In this study, the geomechanical property used to measure rock strength (i.e. unconfined compressive strength) was evaluated by using three principal methods. Critical drawdown pressure (CDP) and sand production rate were also evaluated. Firstly, the use of statistical analysis, secondly, these statistical parameters were combined into a single parameter called rank using the Multiple Statistical Optimization Model. Finally, performance plots of the measured geophysical log and estimated values of the unconfined compressive strength were made to confirm the results of the statistical and ranking methods.

The database consists of forty-three (43) data points obtained from well D4 in the Niger Delta terrain. The best correlation for the Niger Delta reservoir is the Sharma and Singh (2008) correlation. It has a rank of 27.11, and the lowest percentage absolute error (Ea.) of 13.94 which was the best when compared to other correlations evaluated. It had the best performance plot for UCS≤ 75 Mpa and favourably predicted the critical drawdown pressure with 7% deviation from measured CDP. It is recommended to be used in situations where core samples of UCS are not available for the Niger Delta reservoirs as well as other regions of the world where the formation is similar to that of the Niger Delta.

Two wells G-14 and G-15 were evaluated for sand production in this study. The product of their shear modulus and the bulk modulus at all depths considered was less than the threshold value of 8E11psi^2; this suggests the possibility of formation failure in the production life of the reservoir. The possibility of sanding was confirmed by their loading factor value of 2.0 and 2.35 respectively, for well G-14 and G-15. The sand production rates for the two wells show only an average maximum deviation of 5% in all cases investigated but this was below the tolerance of 10% deviation suggested by the model used.

Keywords: Geomechanical properties, unconfined compressive strength, statistical parameters, critical drawdown pressure, loading factor, sand production rate.

ACKNOWLEDGEMENT

To the giver of life and health, God almighty I give thanks.

My sincere appreciation goes to the African Capacity Building Foundation for the scholarship that provided me the opportunity to study in this great citadel of knowledge.

I acknowledge the effort of every lecturer that has impacted knowledge into me, without your contributions I would not be who I am today.

I would like to thank my head of department who also double's as my supervisor, Prof (Emeritus) David O. Ogbe for working tirelessly with me through this research work. His continuous understanding and guidance made this work possible. I am immensely grateful to Onuh Haruna for his assistance in the provision of relevant data used in the work and Arinkoola Akeem Olatunde, Dickson Udebhulu, Korandi Fonso and Engr., Sam Dangana for his assistance and contributions in taking the time to proofread this work and making relevant suggestions.

To my friend Dr, O.R Momoh I say thank you for always being available to offer assistance where and when needed.

My appreciation also goes to the Faculty and Staff of the African University of Science and Technology (AUST) for providing me with this research opportunity and for making the environment bearable during my stay. To all my friends especially, Opara Titus, David Clement for their contributions in various ways and my classmates that made my stay at AUST worth it, God bless you all.

Lastly, my sincere thanks go to my husband Mr. Eric Uzochukwu for his assistance, love, prayers and advice, and for making my dream come true. I love you.

DEDICATION

I dedicate this thesis work to Almighty God for giving me the grace to complete it and to my beloved husband you are the best.

TABLE OF CONTENTS

LIST OF TABLES

LIST OF FIGURES

CHAPTER 1

1.0 GENERAL

1.1 INTRODUCTION

Accurate knowledge of rock mechanical properties (elastics modulus and rock strength) is very important for geomechanical applications such as wellbore stability prediction, sand production and drillability analysis, investigation of the reservoir and overburden compaction behaviour when reservoir pressure depletes. (Woehrl, 2010).

Petroleum reservoir rock composed of materials which ranged from very loose and unconsolidated sand to very well cemented, dense and hard sandstone.

Developing hydrocarbon reserves in the Niger Delta Province, which is predominantly an unconsolidated sandstone terrain, requires grappling with geomechanical problems; so understanding the rock geomechanics of this province will be very important especially for dealing with wellbore stability and sand production.

Unconfined compressive strength (UCS) of rock is regarded as a very important parameter used to address a variety of geomechanical problems ranging from limiting wellbore failure during drilling and to assessing sand problems during production. Accurate laboratory testing is the most dependable approach to obtaining the unconfined compressive strength of rock, but this method is laborious, time-consuming and expensive. In practice, however, a lot of geomechanical problems in reservoirs must be solved when core samples are not available for laboratory testing. Samples of the core required where many wellbore instability problems are encountered are mostly never available for laboratory testing. Empirical relations become almost the only way out to calculate UCS in many situations due to the absence of core samples for laboratory tests.

Sand production is a common problem encountered when producing from a poorly consolidated sandstone reservoir. Clastic formation of the Pliocene and younger tertiary ages are particularly troublesome and sand production and wellbore instability problems maybe expected whenever wells are completed in unconsolidated formations. Sand failures also occur in older formation when in-situ rock strength is reduced by poor completion and production practice. Some of the areas where serious sand production problems have been identified include Nigeria, Trinidad, Indonesia, Egypt, Venezuela, Malaysia, and the Gulf of Mexico. (Osisanya, 2010).

Research work has been carried out over the years in trying to develop detailed methods for predicting the very start of sand production as a function of the strength of the formation, drawdown and reservoir pressure (Wilson et al, 2002). Such models can assist in several aspects of field operations like sand control and management, optimal well completion design and production optimization (Chin and Ramos, 2002).

Generally, the effects of sand production ranges from economics and safety hazards to well productivity; and therefore sand production has been an issue of interest to tackle in the petroleum industry. Some of these effects include erosion of downhole and surface equipment, pipeline blockage and leakage, formation collapse, reduction in productivity, increased intervention costs and complexities, increased shut-in time and other environment issues associated with sand disposal particularly in offshore and swamp locations (Osisanya, 2010). These problems cost the oil industry billions of dollars annually. Therefore, understanding the sand production mechanisms and ability to predict and manage the rate of sand production is beneficial. It is important to predict the possible quantity and particle size distribution of sand, and the frequency of sand produced and transported through the wellbore into the topside facilities. Management of sand production requires a good knowledge of "if the formation will

fail, when the formation will fail and how much sand will be produced from such failure" (Oyeneyin, 2014).

Chang et al. (2006) compiled some empirical correlations that relate formation strength and physical properties in sedimentary rocks. This work extends the Chang et al (2006) methodology to the Niger Delta.

This work is aimed at (i) evaluating some of the existing unconfined compressive strength correlations statistically and ranking them in order to recommend the best correlation that can be applied to evaluate rock strength for the Niger Delta reservoir when core samples are unavailable; (ii) the application of the two best correlations evaluated to calculate the critical drawdown pressure for sand production and (iii) use of a simple and easy-to- use mechanistic model developed by Udebhulu and Ogbe (2015) to predict sand production rate for some Niger Delta wells.

1.2 LITERATURE REVIEW

Related works in the published literature will be reviewed in two sub-sections of this thesis, i.e., geomechanical properties and their applications.

1.2.1 Geomechanical Properties

Some of the mechanical properties of concern for treatment design, reservoir simulation and for maintaining a stable wellbore in a hydrocarbon field are elastic properties, such as Young's modulus (E), Shear modulus (G) and Poisson's ratio (V), (Clark, 1977); (Gidley et al, 1989):- strength properties, which include toughness, tensile and compressive strength; (Bharucha, 2004); poroelastic constant describing the compressibility of the rock matrix compared with the bulk compressibility of rock undergoing specific fluid flow (or migration) conditions. Stress not only controls most aspects of fracture behaviour, but also influences the values of reservoir properties and mechanical properties of the formation. Stress magnitude and orientation have

an effect on the rock properties and the wellbore, and their impact and under in-situ stress regime are important in predicting and managing rock deformation through design, drilling, and production to prevent drilling problems (Fidelis et al., 2016).

In order to design and maintain a stable wellbore requires the acquisition of geomechanical properties data from drilling cores or from wireline logs. Mechanical properties are often measured in the laboratory from cores. Core samples of overburden formations where compressive shear failures occur are needed but are never available for testing prior to the commencement of drilling, also laboratory measurements are expensive and time-consuming.

In order to provide a solution to these problems, geomechanical evaluation and modelling are done based on empirical correlations from measurable physical properties obtained from wireline logs normally available for all offset wells within the field for pre-drilling analysis, modelling and design.(Fidelis et al, 2016)

A lot of correlations and models have been proposed to estimate mechanical properties using some lab measurements and data obtained from wireline logs.

Woehrl, B, (2010) published an empirical correlation for comparison of methods to derive rock mechanical properties from formation evaluation logs.

Mita Sengupta and Keith Katahara (2012) published an empirical correlation for linking physical and mechanical properties of rock.

Rock mechanical properties, which include Poisson's ratio V, shear modulus G, Young's modulus E, bulk modulus K_b, and compressibility, are required for borehole stability evaluation, drillability analysis, and other geomechanical applications. Rock-mechanics testing of core sample is a straight-forward method for obtaining static mechanical properties. Coring

of the sample can, however, provide only discrete data points and can cover only a limited depth range (Horsrud, 2001).

There is an urgent need for techniques that can provide rock properties on a more continuous basis and at a cheap cost. Such techniques can be based on different information obtained from wireline logs, drill cuttings, MWD and seismic inversion, which can be a powerful tool as it provides 3D spatial coverage. (Mita Sengupta and Keith Katahara, 2012).

Empirical correlations have been used to estimate rock mechanical properties from evaluation logs.

Chang et al. (2006) compiled thirty-one (31) different empirical relations for estimating rock strength and evaluated those correlations for a large data set drawn from different areas. Most of the empirical correlations performed poorly for the larger data set, even though they may have performed well for the smaller local data sets from which they were derived.

Azizi and Memarian (2006), published a correlation for estimating geomechanical parameters of reservoir rocks using logs and porosity information based on the data gathered from three wells in Iran and obtained from different formations.

1.2.2 Application of geomechanical properties

Rock geomechanics has become one of the most important support technologies applied in order to develop an efficient plan for the exploitation of hydrocarbons due to the changes induced by petroleum industry activities performed on oil and gas reservoirs. Early applications of geomechanics in the petroleum industry were made to prevent and control sanding and wellbore stability problems of wells (Roegiers, 1995).

Sand prediction, control and management is broad with several publications written with the intent of understanding the critical factors leading to sand production, developing models for

predicting sand production potential and designing various techniques of sand prevention management and control. The goal of most of the publications is to determine whether sand control decisions should be taken during field development. The approaches mostly used are experimental, analytical (models) and numerical simulations. Studies have shown that it is important for the rock strength to be correctly estimated in predicting the sand potential of a given formation. The trend commonly encountered is the evaluation of the strength of rock and formation stress and their application to a failure model.

Zhang et al., (2000) established that the mechanical strength of a formation is very important information required for determining sand production and knowing what type of and control measures to use. Their model presents a method of measuring rock strength such that the restrictions on core testing can be avoided. Tri-axial and hydrostatic tests were carried out to construct the failure envelope. The results of their studies showed that a single normalized failure envelope can be used to characterize sandstone formations making it easy to construct the failure envelope from the knowledge of critical pressure.

Tiab (2014) reported that clastic formations possessing low porosity showed significant rock strength and proposed that porosity can be used as a qualitative measure of rock strength to predict the onset of sanding. He theorized that sand production can be expected if the product of shear and bulk modulus is less than the benchmark value of $8E11psi^2$, where the shear modulus, G and the bulk modulus, K_b are derived accurately from the interpretation of acoustic and density logs.

Willson et al. (2002) came up with a new model for predicting the rate of sand production by using the concept of non-dimensionalised of Loading Factor (LF), Reynolds number (Re) and water production boost factor. They obtained an empirical relationship between loading factor,

reynolds number and the rate of sand production by including the effect of water production. Their proposed definition of sand production rate is SPR = f (LF, Re, water-cut).

Udebhulu and Ogbe (2015) developed a mechanistic model for predicting sand production by linking the static sanding criteria and the dynamic condition for fluidization of the sand produced. The model including the concept of dimensionless quantities associated with sanding the quantities considered included the loading factor (LF), Reynolds number Re, water-cut W and gas-liquid ratio GLR.

1.3 PROBLEM DESCRIPTION

Geomechanical properties are essential for wellbore stability analysis (McLean and Addis, 1990); sand production prediction (Nouri et al, 2006); constraining in-situ stress magnitudes by observing failure at the wellbore (Peska & Zoback, 1995); drilling simulation of penetration rate and drill bit wear (Cooper & Hatherly, 2003).

Technical challenges arising from drilling, coupled with the need to reduce completion and remedial work costs, rock mechanics have found a whole lot of applications especially in addressing problems that have to do with well bore stability and sand production. The crucial step to effective rock mechanics solutions is hidden in obtaining geomechanical properties data like elastic modulus and estimating the strength of rock/ formation (Farquhar et al., 1994).

Unconfined compressive strength of rock (UCS) which measures the rock strength is one of the key parameters required to address various geomechanical problems which ranges from limiting wellbore instabilities during drilling to assessing sanding problems during production. Laboratory-based UCS is evaluated by tri-axial testing on cylindrical samples that are obtained from depths of interest.

In field practice, almost all geomechanical problems associated reservoir drilling and production must be tackled when samples of cores are not present for laboratory testing. At most times, core samples of overburden formations where a lot of wellbore instability problems are experienced are almost never available for testing. The use of empirical relations is often the only way to estimate formation strength in many occasions due to the non-availability of core samples for laboratory tests.

There are multiple choices of rock strength models/relations for diverse rock types in different geological areas, understanding the characteristics/ features of the models and their range of applicability prior to using them is very vital. In order to review the suitability of existing unconfined compressive strength correlations for the Niger Delta, it is important to carry out a critical evaluation of the correlations, which this work will address. The most widely used UCS correlations will be ranked using data from some Niger Delta wells as the benchmark for comparison of the correlations.

The tendency for sand to be produced from an unconsolidated formation increases as the reservoir is being depleted due to a corresponding increase in the effective overburden pressure on the formation with depletion causing the formation to fail at some point. Also as the production rate increases, the drawdown pressure increases which is the difference between the reservoir pressure and the wellbore flowing pressure. This phenomenon tends to draw sand into the wellbore at some point called the critical drawdown pressure. Similarly sand production rate is noted to increase with increasing water-cut.

Sand production is now one of the major challenges being faced by the petroleum industry in the Niger Delta since the formation encountered there is friable and unconsolidated. Consequently, millions of dollars are lost every year due to restricted production rates, well

cleaning and work over operations to mitigate sand production. (Adeyanju and Oyekunle, 2011).

The effects of sand production range from economics and safety hazards to well productivity and therefore has been an issue of interest to tackle in the petroleum industry. (Osisanya, 2010). Saving time and money are the results of proficient sand prediction, control, and management. Though there exists a wide variety of empirical, numerical and analytical sanding prediction models in literature, they require lots of rock mechanics input parameters which are rarely available in field practice. A simple and easy-to- use mechanistic model will be used to predict sand production that is applicable to poorly consolidated clastic terrain.

1.4 OBJECTIVES AND APPLICATION OF STUDY

The objectives of this study include:

- To evaluate existing correlations for estimating geomechanical properties especially those used to measure rock strength (unconfined compressive strength) for its usability in the Niger Delta.
- To investigate different methods for choosing the best correlation i.e. statistical error analysis, ranking, cross plot (graphical analysis) and multiple statistical optimization models.
- To use a mechanistic model to predict sand production for the Niger Delta wells.
- To validate the model by comparing computed results from the model with field data obtained from Niger Delta wells.

The applications of this study include:

- Sand Monitoring Strategy
- Completion Design
- Perforation Strategy

- Wellbore Stability during drilling
- Field Economics

1.5 ORGANIZATION OF THESIS

The thesis is divided into five chapters. Chapter one gives a brief introduction and literature review on the subject matter, it also states the objectives and application of the study. Chapter two presents a theoretical background of geomechanical properties with related correlations and their application. Chapter three describes the methodology used to evaluate the correlations and sand production prediction. Validation of field data, statistical evaluation and analysis of the results obtained is shown in chapter four. Chapter five provides the conclusions and recommendations of the thesis.

CHAPTER 2

2.0 THEORETICAL BACKGROUND OF GEOMECHANICAL PROPERTIES, CORRELATIONS AND APPLICATION

2.1 DESCRIPTION OF THE STUDY AREA

The study area which is the oil-rich Niger Delta region (Figure 2.1) lies in the Nigerian sector of the Atlantic Ocean. This sedimentary basin is a clastic environment dominated by sands and shales. This area is associated with rifting that actually gave rise to the development of the Benue Trough. The delta consists of three major lithostratigraphic formations, namely, the Akata, Agbada and Benin lithology. The source rock of hydrocarbons in the area is believed to be the Akata Formation which is a marine deposit that consists of basically clays. It is preceded by the sandstones and clays of the hydrocarbon-rich Agbada Formation. Overlying the prolific Agbada Formation is the Oligocene to Recent Benin Formation which comprises of medium to high coarse-grained sandstones. Therefore, the regional lithological outlook of the area is that of alternating successions of sands and shales (Table2.1).

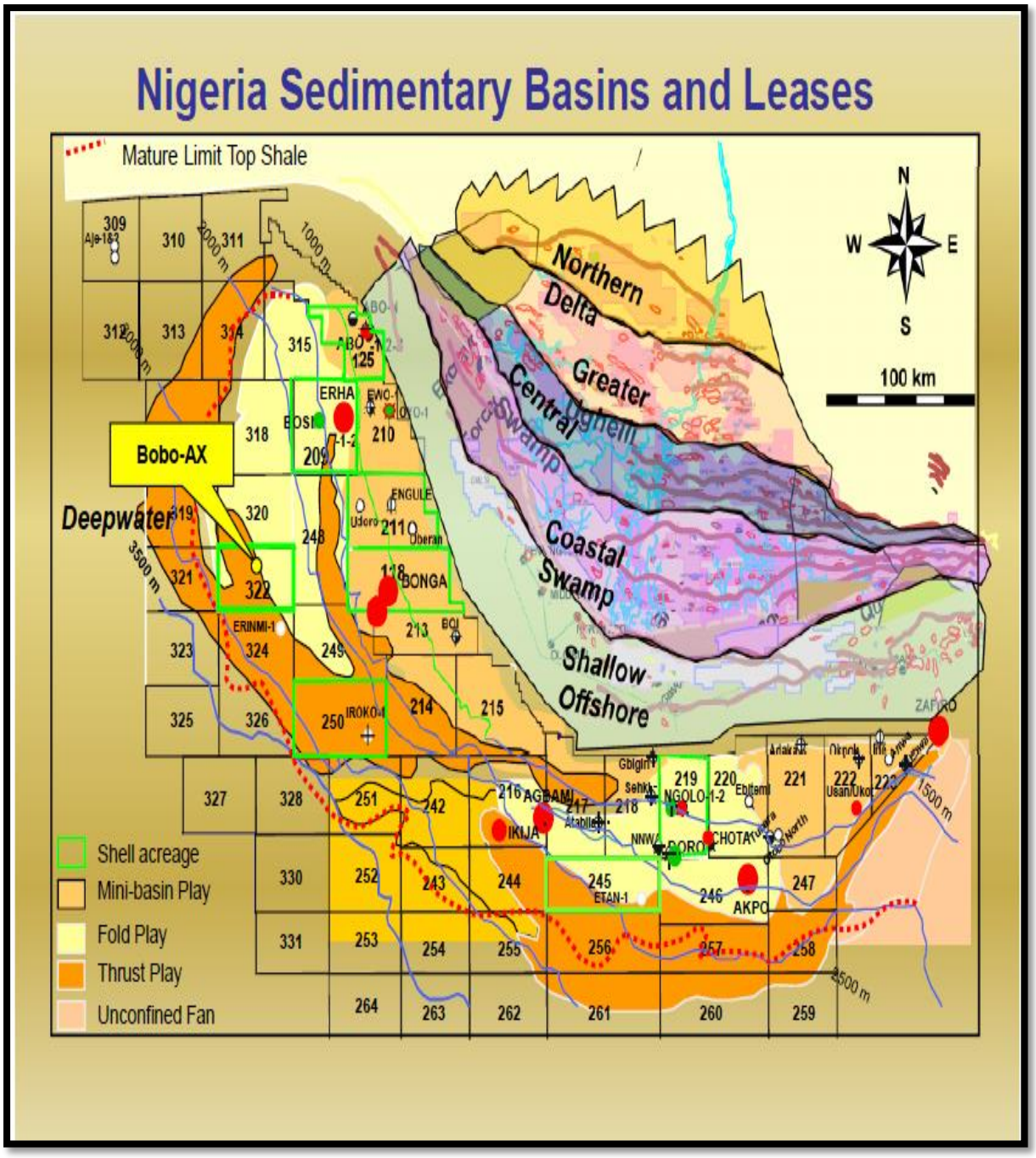

Figure 2.1: Map Showing sedimentary basin and leases (Source: Onuorah et al, 2014)

Table 2.1: Major Geologic Units of the Niger Delta (Source: Onuorah et al, 2014)

Geologic Member	Constituent rock types
Alluvium	Gravel, sand and argillaceous deposits
Fresh water swamp	Sand, gravel, silt and clay
Coastal swamp	Sand (various grains size), clay silt
Beach ridges	Sand, clay and silt
Deltaic plain	Sand, clay and silt
Coastal plain sand (Benin formation)	Medium to coarse grained sand with clay
Agbada formation	Main reservoir, sand, clay, silt

2.2 WELL LOGS

Well logs are used for in-situ measurement of rock properties such as Porosity, Net pay intervals, Water saturation, Permeability estimates, and lithological properties. The logs provide petrophysical data recorded continuously versus depth, but do not measure directly the parameters that are required for a rock mechanical analysis. A brief description of the well logs used in this thesis is presented in the following section.

2.2.1 Density Log

Density log is a well logging tool that can provide a continuous record of a bulk density along the length of a borehole. It uses gamma rays in gathering data about subsurface formations. The bulk density measure is a function of the density of the minerals forming rock and the fluid enclosed in the pore spaces. The tool consists of a radioactive source and a single detector, but this configuration is susceptible to the effects of the drilling fluid. Density logging now conventionally uses two or more detectors. In a two detector configuration, the short-spaced detector has a much shallower depth of investigation than the long-spaced detector so it is used to measure the effect that the drilling fluid has on the gamma ray detection. This result is then

used to correct the long-spaced detector. The density log is used to determine porosity as indicated in the following equation:

$\rho_b = \rho_{ma}(1- \emptyset) + \rho_f + (\emptyset)$ …….. (2.1)

Where

ρ_b = Bulk density log response

ρ_{ma}= Density of matrix mineral grains

ρ_f = Density of fluid in the pore space

$\emptyset$ = Porosity, fraction

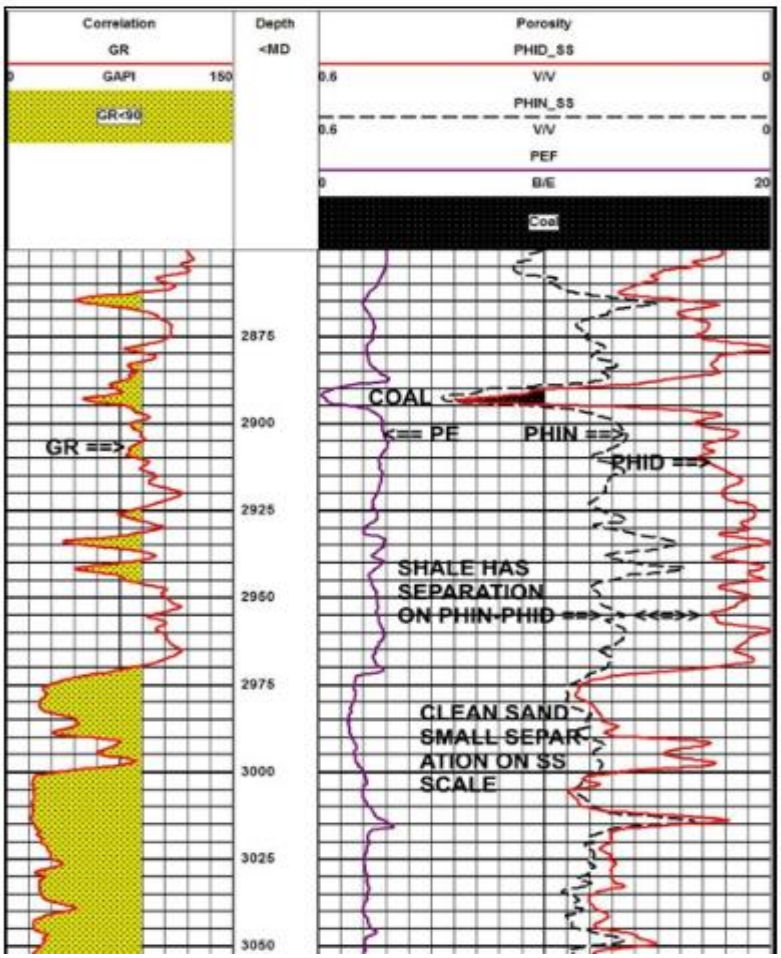

Figure 2.2: Diagram Showing Density Log (spesc2000.net/01-crainrules.htm)

2.2.2 Acoustic (Sonic) Log

This is a well logging tool used to provide formation's interval transit time, Δt, which is a measure of a formation's capacity to transmit seismic waves. Geologically, this formation capacity varies with lithology, the texture of the rock and mostly decreasing with an increasing effective porosity. This means that a sonic log can be used to calculate the porosity of a formation if the seismic velocity of the rock matrix and pore fluid are known.

The velocity is calculated by measuring the travel time from a piezoelectric transmitter to the receiver, normally with the units' microsecond per foot, a measure of slowness. Since there is variation in the drilling mud thickness. The acoustic energy emitted by a transmitter travels through the formation is detected by multiple, one near and one far. Time difference in receiving an acoustic pulse is measured at each receiver which is shown by a white dash line in Figure 2.3 below. The difference in travel path is a small distance within the rock formation (yellow arrow in Figure 2.3).

Some of the areas for the application of Sonic include:

- Formation evaluation (porosity, gas detection, fractures, permeability, (cement bond log).
- Geophysical interpretation (synthetic seismograms, vertical seismic profiling, Amplitude-versus-offset analysis)
- Mechanical property analysis (sanding, fracture height, and wellbore stability)

$$\Delta t = \Delta t_{ma}\,(1 - \emptyset) + \Delta t_f\,(\emptyset) \quad \text{..... (2.2)}$$

Where

Δt = Sonic travel time log response

Δt_{ma} = Sonic travel time for matrix mineral grains

Δt_f = Sonic travel time for fluid in the pore space

$\emptyset$ = porosity, fraction

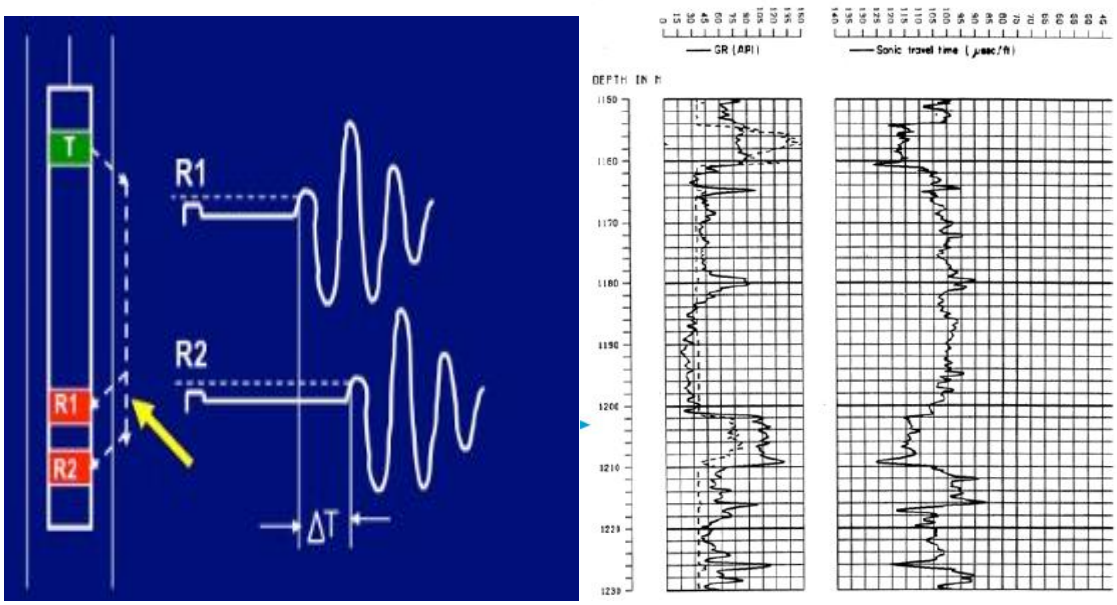

(a) (b)

Figure 2.3: Diagram Showing (a) Sonic Log tool and (b) Sonic log (Courtesy of ExxonMobil; Schroeder, 2004)

2.2.3 Resistivity Logging

The resistivity of a substance is its ability to impede or oppose the flow of electric current through a material or substance. Formation resistivities usually fall in the range from 0.2 to 1000 ohm-meters.

Resistivities higher than the 1000 ohm-meter are rare in permeable formations. In a formation containing hydrocarbon, both components of the hydrocarbon are electrical insulators. Resistivity is related to the formation factor, brine resistivity, and water saturation which in turn depends on the true resistivity of the formation variables. One major importance of

resistivity is that it is required to determine mainly the volumetric concentration (saturation) of hydrocarbon in a subsurface formation.

2.3 Geomechanical Properties and Correlations

A lot of problems occur repeatedly during oil and gas well drilling operations such as sloughing shale, stuck drill pipe, etc. Normally, the first attempt to resolve such problems is based on the experience of the petroleum engineer. If all methods fail to solve such problems, a rock mechanics study is considered to be the last remedy. At this stage, rock mechanics analysis will be difficult due to the lack of data and rock samples to carry out such analysis; therefore, back analysis may be the only solution if new offset wells are not drilled. Thus, rock mechanics must be considered from the beginning, during drilling, and a rock mechanical database must be established to assist in solving new problems (Al-Awad, M. N. J., 1992). Wellbore instability during drilling, for example, costs the industry around $400–500 million per year (Bol, G.M., 1998). On the course of producing reservoir fluids over a long period, many problems related to rock mechanics may be encountered such as sand production, perforation instability, subsidence, mechanical damage, etc. In order to solve any of the previously mentioned problems that may be encountered, rock failure criterion and rock mechanical properties must be determined. To evaluate the mechanical properties of the rock, a sufficient number of rock specimens are needed in addition to a costly tri-axial testing set-up. Therefore, simple correlations are needed to estimate rock mechanical properties using a limited number of rock samples and inexpensive and rapid tests.

Rock deformation mechanisms are involved in the petroleum reservoir formations and the overlaying strata. Some programs carried in the formation in which rock deformation may occur include: drilling, production, fracturing, stimulation, or enhanced oil recovery. Understanding of the rock-stress relationship can solve many reservoir problems and avoid the cost of remedial/work over programs (Musaed N. J. Al-Awad, 2012).

Production of the reservoir as well as injection programs affects the levels of subsurface stress during the life of an oil and or gas field and can cause severe challenges in field development and production, such challenges include: compaction and subsidence, changes in reservoir permeability, fault reactivation, water breakthrough, and breaches in cap rock/trap integrity. In the reservoir and the overburden, these geomechanical changes, combined with complex geology, can affect completion stability and cause casing collapse and sanding across the field. Figure 2.6 shows various geomechanical problems that are encountered in the reservoir upon production from field exploration to abandonment.

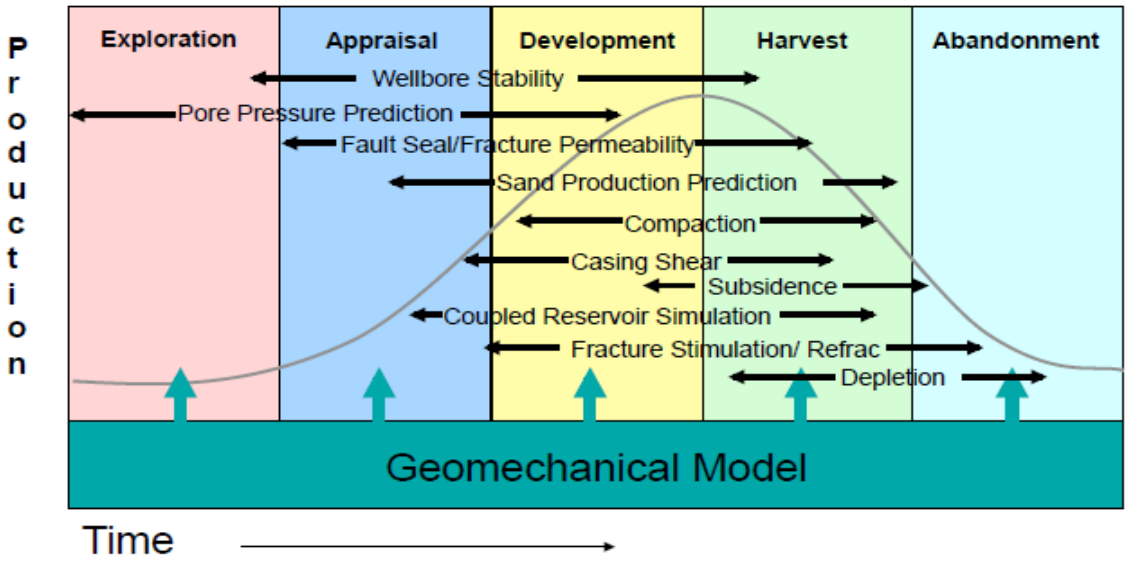

Figure 2.4: Geomechanics through the Life of a Field (Source: Reservoir Geomechanics Stanford Online, 2016).

2.3.1 Stress Analysis

When a rock body is subjected to an external load, internal stresses are created. If these stresses are strong enough, the rock alters in shape. Deformation refers to changes in shape accompanied by a change in volume. Three basic internal stress conditions are identified which include compressive, shear, and tensile stress, as illustrated in Figure 2.4 Compressive stresses takes place when external forces are geared toward each other along the same plane. If the

external forces fore mentioned are parallel and positioned in the opposite directions along the same plane, tensile stress develops. When the external forces are parallel and directed in opposite directions, but in different planes then shear stress develops.

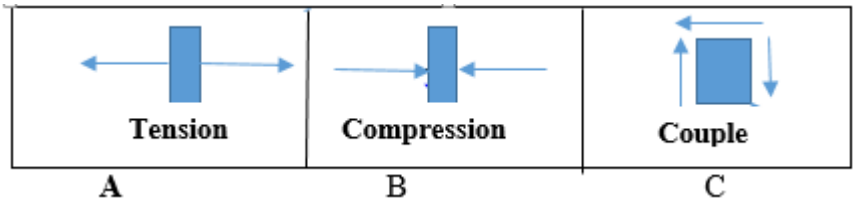

Figure 2.5: Representation of Tension, Compression, and Couple (Adapted from Tiab and Donaldson, 2004).

It is possible to prove that there is one set of axes with respect to which all shear stresses are zero and the normal stresses have their highest values. The three mutually perpendicular planes where these requirements exist are called the principal/main planes, and the principal stresses are the three normal stresses on the planes (Figure2.8).

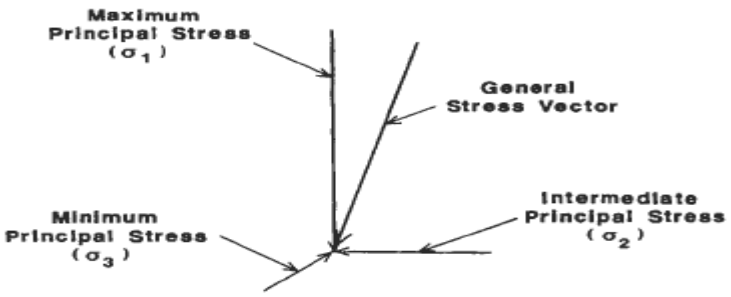

Figure 2.8: Principal Stresses acting on a point (Source: Tiab and Donaldson, 2004).

2.3.2 Rock Deformation

Stress and strain relationship for reservoir rocks is determined by a large number of factors. Some of these factors are: what the rock is made up of, the lithology of rocks, their degrees of cementation and changes in the rock, type of cementing material, quantity and type of fluids in the pore space, rock matrix and fluid compressibility, porosity and permeability of rock, and the reservoir pressure and temperature. Many of these factors are interrelated, and their singular and combined effect on the relationship between stress and strain can only be measured in the laboratory, using a representative rock sample from the reservoir and subjecting the test

parameters to some control to accurately simulate the in-situ condition. Three measuring and loading techniques used for rock deformation tests are hydrostatic, uniaxial, and tri-axial technique.

2.3.3 Shear Modulus

Shear modulus (G) or modulus of rigidity is the ratio of applied shear stress to shear strain, it is given by:

$$G = \frac{\boldsymbol{shear\ sress}}{\boldsymbol{shear\ strain}} = \frac{\boldsymbol{\tau}}{\boldsymbol{\gamma}} \quad \ldots\ldots (2.3)$$

For a rock that has similar properties and identical in all direction, homogenous, and elastic the shear modulus is by (Amaefule et al, 1993):

$$G = 1.348 \times 10^{-2} \frac{\rho b}{\Delta ts^2} \quad \ldots\ldots (2.4)$$

Where G is the shear modulus of the rock and ρb is density and Δts is the shear wave interval travel time

2.3.4 Bulk Modulus

Bulk Modulus (Kb) represents the ratio of changes in the average of the three principal stresses to the changes in rock volume. Or is the ratio of change in hydrostatic stress to the corresponding volumetric strain:

$$K = \frac{\Delta P}{\Delta V/Vo} \quad \ldots\ldots (2.5)$$

Where Δp is the change in hydrostatic pressure, ΔV is the change in volume, and V_o is the original volume. The bulk modulus is the inverse of rock matrix compressibility, Cr:

$$K = \frac{1}{Cr} \quad \ldots\ldots (2.6)$$

For a rock that has similar properties and identical in all direction, homogenous, and elastic the bulk modulus is by:

$K_B = 1.348 \times \rho_b[\frac{1}{\Delta tc^2} - \frac{4}{3\Delta ts^2}]$ …… (2.7)

2.3.5 Young's Modulus

This is a measure of the property of the rock to resist deformation.

The Young's modulus is the ratio of compressive/ tensile strength to compressive/tensile strain which for a rock that has similar properties and identical in all direction, homogenous, and elastic the modulus is given as (Azizi and Memerian, 2006):

$E = \frac{9GK_B}{3K_B + G}$……..……..…… (2.8)

2.3.6 Poisson's Ratio

Poisson's ratio (ν) can be defined as the ratio of the lateral strain to longitudinal strain when a longitudinal stress is applied. (Tiab and Donaldson, 2004)

$V = -\frac{\varepsilon_{lat}}{\varepsilon_{ax}} = \frac{\Delta d/d_o}{\Delta l/L_o}$ ……. (2.9)

Where: do = original diameter of the cylindrical core sample.

Δd = change in diameter.

Lo = original length of core.

ΔL = change in length.

ε_{lat} = strain in the lateral direction

ε_{ax} = strain in the axial direction.

Poisson's Ratio for a homogeneous, isotropic and elastic rock is given as:

$$PR = v = 0.5 \left[\frac{(\frac{DTS}{DTC})^2 - 2}{(\frac{DTS}{DTC})^2 - 1}\right] \quad \text{(2.10)}$$

The four elastic constants (2.1, 2.3, 2. 6 and 2. 7) are not independent of each other, and if any two are known it is possible to derive the others. (Tiab and Donaldson, 2004)

$$G = \frac{E}{2(1+v)} \quad \text{(2.11)}$$

$$K = \frac{E}{3(1-2v)} \quad \text{(2.12)}$$

$$G = \frac{9KG}{3K+G} \quad \text{(2.13)}$$

$$V = \frac{3K-2G}{2(3K+G)} \quad \text{(2.14)}$$

2.3.7 Rock Strength

Rock strength is the ability of rock to withstand stress without yielding. It is affected by the mineral content of the rock fragments and by the behaviour of the particle contacts. Deposition, diagenesis, and catagenesis are the factors that give the rock its properties, later they are modified by folding, faulting, fracturing, jointing, and weathering. As a result, the strength of rocks reflects their geological background. Rock strength is evaluated by two widely used laboratory methods which include: unconfined compressive strength tests, and tri-axial tests. Unconfined compressive strength (UCS) as defined by encyclopedia 2013, simply refers to the strength of a reservoir rock when a compressive force is applied in one direction without lateral constraint.

Unconfined compressive strength tests are used to determine the ultimate strength of a rock, i.e., the highest value of stress reached before the formation fails. The uniaxial strength is one of the simplest measures of strength to obtain. (Tiab and Donaldson, 2004)

2.3.8 Unconfined Compressive Strength of Sandstone Reservoirs

The major contributor to sanding problems and casing collapse in many oil and gas fields is compressive wellbore failure. This type of failure occurs when the pressure at the wellbore exceeds the rock or formation strength, especially in unconsolidated and weakly cemented rocks where stimulation programs have made the rock cement weak. (Ohen, 2003)

Almost all proposed models for determination of rock/formation strength from geophysical logs use one or more of the following parameters:

• P-wave velocity (Vp) which is the reciprocal of interval transit time ($\Delta t = Vp^{-1}$), and is directly measured.

• Young's modulus (E), which is obtained from velocity and density measurements.

• Porosity (ϕ), which is generally obtained from measurement of density assuming rock/ formation matrix and fluid densities.

Equation (1)–(11) in Table2.2 presents a number of relationships in common practice (both published and patent) for evaluating the unconfined compressive strength of sandstones from the geophysical log. These correlations were derived for case studies carried out for markedly different types of rocks in different geological locations of the world. General comments such as the regions and/or the general rock properties suitable for each equation are indicated in Table 2.2. If no reference is shown in Table 2.2, the given empirical relation is unpublished. Equations 1 through to 3 utilize P-wave (Vp) or are expressed equivalently as interval transit time Δt measurements from well logs. Equations (5) – (7) utilize both density and V_P data; and

Eq. (4) utilizes p- wave velocity V_P, density ρ, Poisson's ratio ν (which requires V_s measurement) and clay volume V_{clay} (from gamma ray logs). Equations (8) and (9) utilize Young's modulus, E, derived from V_P, Vs, ρ, and equation (10) and (11) utilize porosity derived from log measurements to estimate UCS and Eqs.12-21 utilizes p- wave velocity Vp.

Table 2.2: Empirical Relationships between Unconfined Compressive Strength (UCS) and Physical Properties of Sandstones

Correlation number	UCS (Mpa)	Regions where developed	General comments	Reference
(1)	0.035Vp – 31.5	Thuringia, Germany	-	Freyburg(1972)
(2)	1200exp(-0.036Δt)	Bowen basin, Australia	Fined grained, both consolidated and unconsolidated sandstones with all porosity ranges	McNally (1987)
(3)	$1.4138\times10^{7}\,\Delta t^{-3}$	Gulf coast	Weak and unconsolidated sandstones	
(4)	$3.3\times10^{-20}\rho^{2}Vp^{4}[(1+v)/(1-v)]^{2}$	Gulf coast	Applicable to sandstones with UCS > 30 Mpa	

	(1-2v)[1+0.78V_{clay}]			
(5)	1.745×10^{-9} ρV_p^2-21	Cook inlet, Alaska	Coarse grain sandstone and conglomerates	Moos et al (1999)
(6)	42.1 exp($1.9\times10^{-11}\rho Vp^2$)	Australia	Consolidated sandstone with 0.05 < Ø< 0.12 and UCS > 80Mpa	
(7)	3.87exp(1.14×10^{-10} ρV_p^2)	Gulf of Mexico		
(8)	46.2exp(0.027E)	-	-	-
(9)	2.28+ 4.1089E	World wide	-	Bradford et al (1998)
(10)	$254(1- 2.7Ø)^2$	Sedimentary basins Worldwide	Very clean, well-consolidated sandstones with Ø < 0.3	Vernik et al (1993)
(11)	277exp(-10Ø)	-	Sandstone with 2<UCS<360Mpa	

			and $0.002 < \emptyset < 0.33$	
(12)	$2.45V_p^{1.92}$			Militzer and Stoll(1973)
(13)	$10^{0.385Vp - 0.283}$			Golubev and Rabinovich (1976)
(14)	$1277\exp(-\frac{11.2}{Vp})$			McNally(1978)
(15)	$36V_p - 31.2$			Goktan (1988)
(16)	$35.5V_p - 55$			Tugrul and Zarif(1999)
(17)	$9.95V_p^{1.21}$			Kahraman(2001)
(18)	$31.5V_p - 63.7$			Yasar and Erdrogan (2004)
(19)	$22.03V_p^{1.247}$			Sousa et al (2005)
(20)	$64.2V_p - 117.99$			Sharma and Singh (2008)
(21)	$36V_p - 45.37$			Sharma and Singh (2010)

(22)	$258e^{-9\emptyset}$		Use for porosity up to 30%. Unconfined compressive strength of the in-situ undamaged sand- Stones	Source (Tiab and Donaldson,2004)
(23)	$f(\theta_f)\frac{\rho_b^2}{\Delta t_s^2}[\Delta t_c^2 - \frac{4\Delta t_s^2}{3}]$ g(V_{sh})		Where f=factor, ($\theta_f =$ frictional angle	Sarde et al(1993)
(24)	0.087× $10^{-6}EK_b[0.008V_s$ $_h+ 0.0054(1- V_{sh})]$		For sand strength limit, the internal friction angle $\emptyset_f = 30^\circ$	Coates and Denoo (1981) Bruce (1990)

2.3.9 In-Situ Stress Distribution

Strength and elastic properties relationship are measured at laboratory conditions and those which exist at wellbore depths have not been well understood and treated. However, several theories describing the induced stress distribution around a drilled hole are available. The total vertical stress δ_{OB}, which is normally equivalent to the maximum principal in-situ stress, can

evaluate from well logs. The minimum principal horizontal stress, σ_{Hmin}, can be approximated, sometimes with precision, by the instantaneous shut-in pressure measured during or after a fracturing job. In areas without tectonic activities, the total maximum horizontal stress, $\sigma_H$max, is approximately equal to the total minimum horizontal stress, $\sigma_H$min. In the more general case ($\sigma_H$max > $\sigma_H$min); however, these approximations are invalid, and the relation put together by Breckels and van Eekelen appear to be very useful.

The following two correlations are valid for normally pressured sands:

- For Depth, D ≤5 11,500 ft:

  $\sigma_{HMin} = 0.197D^{1.145}$ ……. (2.15)

- For D > 11,500 ft:

  $\sigma_{HMin} = 1.167D - 4596$ ……. (2.16)

- The minimum horizontal stress in abnormally pressured formations in the Gulf Coast region can be estimated as:

  For D ≤5 11,500 ft:

  $\sigma_{HMin} = 0.197D^{1.145} + 0.46(P_p - P_{pn})$ ……. (2.17)

Where $P_{pn,}$ is the normal pore pressure value of 0.465psi/ft

- For D > 11,500 ft.:

  $\sigma_{HMin} = 1.167D - 4596 + 0.46(P_p - P_{pn})$ …….. …….. (2.18)

2.3.10 Stress Relationship at the Wellbore

The simple model, which relates the maximum tangential stress $\sigma_{\theta max}$ to the principal stresses σ_{Hmax} at the wellbore, is given as:

$\sigma_{\theta max} = 3\sigma_{Hmax} - 3\sigma_{Hmin} - P_{bh}$ …….…. …….. (2.19)

The maximum tangential stress $\sigma_{\theta max}$ occurs in the direction of the least principal stress σ_{Hmin}. The axial stress is estimated as:

$\sigma_{axial} = \sigma_{oB} + 2v\ (\sigma_{Hmax} - \sigma_{Hmin})$ …… (2.20)

Where v is the static Poisson's ratio of the formation rock. Equations 2.16 and 2.17 are valid only if the pore pressure is the same throughout the formation. To incorporate the changing pressure profile of the pore and the pore elastic term, Haimson and Fairhurst (1997) developed the following correlation:

$\Delta\sigma = \alpha[\frac{(1-2v)}{(1-v)}(P_{wb} - P_{p)}]$……... (2.21)

Where $\propto$ is the Biot coefficient and Pwb is the pore fluid pressure just behind the wellbore.

2.4 Sand Production

Sand production is one of the major challenges being faced by the petroleum industry in the Niger Delta, as millions of dollars are lost every other year due to restricted production rates, well cleaning and remedial work. (Adeyanju and Oyekunle, 2011).

Schlumberger (2013) defined sand production as the movement of formation sand caused by the flow of reservoir fluids. Sand production actually starts when there is failure of rock around the perforations, and the fluids can push the loose sand grains into the wellbore. (Eriksen, et al. 2001). Sand production is a process that develops progressively in three stages: firstly, the rocks surrounding an open hole fails or perforation from which free sand grains are generated,

secondly, there is disaggregation of sand particles from failed material/rock, and finally there is transport of those free sand grains by the effluents/fluid into the wellbore and up to the surface (Sunday and Andrew 2010).

Depletion and drawdown fail the medium under shear, tensile or volumetric failure mechanisms or a combination of both mechanisms (Nouri et al., 2003). The production of formation sand usually starts during the early or later stages in the life of the reservoir when pressure depleted or water breaks through. Sand production erodes downhole equipment and surface facilities, production pipeline blockage and leakage, creates additional need for waste disposal which could be a problem in areas of strict environmental regulations, leads to formation subsidence in severe cases and generates more frequent need for remedial work and well intervention. These effects can be viewed as both economic and safety hazards in the petroleum industry.

2.4.1 Causes of Sand Production

Some of the factors influencing the tendency of a well to produce sand can be categorized into rock strength effects and fluid flow effects. Production of sand particles consists of formation fines and load support solids. The production of formation fines which is not considered as part of the formations mechanical framework is useful because they can move freely through the formation instead of plugging it. Production rates are often kept to low levels so as to avoid the production of the load bearing particles, in many cases, however, low production rates are uneconomical for the industry. These factors include:

1. The degree of consolidation: The ability to keep the perforation tunnels open is closely tied to how strongly the individual sand grains are bound/cemented together. The cementation of sandstone is actually a secondary geological process/mechanism and as a rule of thumb, older sediments tend to be more consolidated than younger sediments. This indicates that sand production is usually a problem when producing hydrocarbon from shallow (not

deep), geologically younger tertiary sedimentary formations/rock. Such younger formations are located in the Gulf of Mexico, California, Nigeria, France, Venezuela, Trinidad, Malaysia, Egypt, China, Brunei, Italy Indonesia, etc. Young Tertiary formations often have little cementation bonding the sand grains together and these formations are generally referred to as being unconsolidated. Compressive strength is the mechanical property of rock that is related to the degree of consolidation. Unconsolidated sandstone formations usually have a compressive strength that is less than 1,000 psi (Completion tech., 1995).

2. Production rate: Increasing the production rate creates large fluid pressure gradient near the perforation which tends to draw sand into the wellbore. Generally, as reservoir fluids are being produced pressure differential and frictional drag forces are created that can combine to exceed the formation compressive strength. This shows that there is a critical flow rate of production below which pressure differential and frictional drag forces are not strong enough to exceed the rock compressive strength and cause sand production. The critical flow rate of a well may be determined by gradually increasing the production rate until sand production is noticed. One technique used to reduce the production of sand is to choke the flow rate down to the critical flow rate where sand production does not occur or has an acceptable tolerance. In many cases, this flow rate is significantly below the acceptable production rate of the well which is not economical (Completion tech., 1995).
3. Pore pressure reduction: production of fluid from the reservoir over time depletes the reservoir pressure resulting in pore pressure reduction. As the pressure in the reservoir is decreased throughout the active life of a well, some of the support for the overlying rock is removed. Lowering the reservoir pressure gives rise to an increasing amount of stress on the rock/formation i.e., the effective overburden pressure increases (Completion tech., 1995). The formation sand particles may break loose from the matrix at some time in

reservoir life which could be produced along with the reservoir fluids. In severe cases, the formation might subside if the effective stress exceeds the formation strength due to compaction of reservoir rock from a reduction in pore pressure.

4. Reservoir fluid velocity: The frictional drag force exerted on the sand grains is created by the flow of reservoir fluid. This frictional drag force has a direct relationship to the velocity of fluid flow and to the viscosity of the formation/ reservoir fluid being produced. The higher the reservoir fluid viscosity the greater the frictional drag force on the sand grains will be than in a reservoir fluid with a lower viscosity. Viscous drag causes sand to be produced from heavy oil reservoirs which are low API gravity oil, they have high viscosity even at low flow velocities (Completion tech., 1995).
5. Increasing water production: Increase in water-cut increases sand production or as the reservoir starts producing water sand production begins. These occurrences can be explained by two mechanisms. In a typical water-wet sandstone formation, there is grain-to-grain cohesiveness which is provided by the surface tension of the connate water surrounding each sand grain. At the beginning of water production or water break through the connate water tends to adhere to the water produced, giving rise to a reduction of the surface tension forces and later result in a reduction in the grain-to-grain cohesiveness. Sand arch stability around the perforation has been shown to be constrained greatly by the production of water resulting in the production of sand. A sand arch is a hemispherical cap of interlocking sand grains that is stable at constant drawdown and flow rate preventing sand production (Jon Carlson et al., 1992). Another mechanism by which water production affects sand production is directly linked to its effects on relative permeability. As the water-cut increases, the relative permeability to oil decreases. It results in an increase in the pressure differential which is required to be equal to the produced oil at the same rate. When the pressure differential is increased near the wellbore it creates a greater shear force

across the formation sand grains. Therefore, higher stresses can lead to instability of the sand arch around each perforation and therefore leading to sand production (Completion tech., 1995).

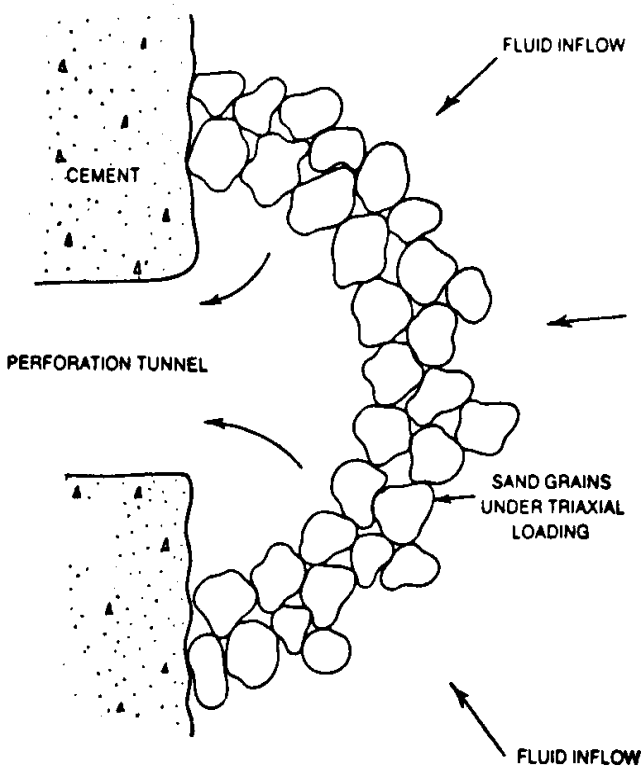

Figure 2.6: Geometry of a Stable Arch Surrounding a Perforation (Source: Completion tech., 1995)

2.4.2 Effect of Sand Production

The effects of sand production are often dangerous to the productivity of a well in the long run. Downhole equipment might be blocked or damaged and/or surface facilities disabled.

1. Erosion of downhole and surface equipment: production of sand at high velocity can erode surface and downhole equipment leading to frequent maintenance and replacement of such equipment. Potential sites for downhole erosion are blast joints, tubing opposite perforations, screens or slotted liners not packed in the gravel pack installation. The most hazardous situation is a high-pressure gas containing sand particles expanding through the

surface choke. For some equipment failures, a rig assisted workover and remedial work will be required to repair the damage (William and Joe, 2003).

Figure 2.7: Surface choke failure due to erosion by formation sand (Source: Completion tech., 1995

Figure 2.8: Eroded piston head (Source: Han et al., 2011)

2. Formation subsidence: the cumulative effect of production of formation sand is the collapse of the formation. Over a long period of time, large volumes of sand will be produced at the

surface creating a void/space behind the casing. This void becomes bigger as more sand is produced. Formation sand or shale above the void may collapse into it as a result of lack of material for support. In formations with high clay content or a wide range of grain sizes, the sand grains re-position themselves to create a low permeability than was initially present. In situations where the overlying shale collapses, complete loss of productivity is likely. The collapse of the formation is very important if the formation is totally or partially filled with formation sand in the perforation tunnels. Even a small amount of formation material filling the perforation tunnels will lead to a reasonable increase in pressure drop across the formation near the well bore for a given flow rate (Completion tech., 1995).

3. Accumulation in surface equipment: if the production velocity of the reservoir fluid is sufficient to carry sand up the tubing to the surface, sand particles often settle in surface facilities of separators, heaters, pumps, condensers etc. As the sand accumulation builds to reasonable volume in these facilities, equipment clean-up becomes almost inevitable. This problem may lead to deferred production (i.e. well is shut-in) and additional costs are incurred as a result of the clean-up activity. The separator production capacity is reduced if it is partially filled with sand. This is as a result of its reduced ability to handle gas, oil, and water.
4. Subsurface accumulation: in cases when the production flow velocity is not enough to carry the sand particles to the surface, the sand accumulates in the casing or bridges off in the tubing; with time the production region might be filled with sand. The production rate for such wells will be reduced which might eventually cease as the sand accumulation makes it very difficult for production to continue. Workover is often required at such times for the well to resume production and if the sand production is continuous, regular well clean out operations will be required. This increases maintenance cost and lost production time which in turn reduces the rate of returns from the well.

5. Disposal of sand produced: Sand produced at the surface of disposal constitutes a problem especially in areas where there are strict environmental laws. Offshore processing systems may not satisfy anti-pollution regulation of the separated sand so the sand needs to be transported onshore for disposal which constitutes additional production cost.

2.4.3 Sand Prediction

It is important for the completion engineer to know under what conditions a well produces sand in order to predict what type of sand control mechanism will be required. Sand prediction is usually carried out at the initial stage of reservoir field development. It comprises the development of completion design, reservoir management strategy, perforation strategy, sand monitoring strategy, planning of the surface facilities and field economics. Sand prediction is not an easy one as the process is more of art than a science. At best, the performance of close by offset wells are observed or a well which completed conventionally and is flowed to observe if sand will be produced. Most of the published techniques to predict the onset of sanding can be categorized into four basic methods: using Field observations and well data (Empirical), Laboratory simulation method, Numerical method and Analytical method (Qui et al, 2006). Most times two or more of these approaches are used in combination for prediction.

2.4.3.1 Empirical Methods Using Field Observations and Well Data

This approach uses a correlation between sand production well data and field operational parameters for sand prediction. To evaluate the sanding potential and to establish a benchmark for sanding or no sanding, one or a group of parameters are used. This is due to the fact that practically it is difficult to monitor and record several years' worth of data for all the wells involved in a particular study (Veeken et al., 1991). Parameters used include porosity, drawdown or flow rate, compressional slowness etc. Veeken et al., (1991) presented the following list of the parameters that may influence sand production they include:

A. FORMATION:

Rock

- Strength (formation strength)
- Vertical and horizontal principal stresses
- Depth (influences strength, stresses around it and pressures)

Reservoir

- Field pore pressure (changes during depletion)
- Permeability
- Fluid composition (consists of gas, oil, water)
- Drainage radius
- Reservoir thickness
- Heterogeneity

B. COMPLETION

- Wellbore orientation, wellbore diameter
- Completion type (open hole or perforated tunnel)
- Perforation policy (height, size, density, phasing)
- Sand control (screen, gravel pack, frac pack chemical consolidation or others)
- Completion fluids, stimulation (acid volume and type)
- Size of tubular (dimension)

C. PRODUCTION

- Fluid flow rate
- Drawdown pressure
- Flow velocity
- Skin

- Bean-up/shut-in policy
- Artificial lift
- Depletion (pressure)
- Water/gas coning and cumulative sand volume.

Field data based sand prediction tools use only one parameter in its simplest form. Examples include avoiding porosities higher than 30 percent (Bellarby, 2009); using a cut-off depth criterion for the installation of sand control measures in several deltaic environments: usually, sand control devices are not installed below a certain depth. A depth of 12,000ft and 7,000ft was recommended by Tixier et al (1975) and Lantz et al (1966) respectively; the depth criteria is regionally dependent. Also applying a compressional sonic wave transit time **(Δt_c)** below which sand control is not required; the limit $\Delta \mathbf{t_c}$ is also field or regionally dependent and may vary from 90 to 120µs/ft (Veeken et al, 1991). Tixier et al., (1975) derived a log-based method using mechanical properties log to predict sanding. A limit value for the sonic and density log-derived parameter ratio of shear modulus, G to the bulk compressibility, C_b ratio (G/C_b) was established. When it G/C_b exceeds $8*10^{11}$ psi ^{2}, no sanding problem is expected. At ratios less than $7*10^{11}$ psi ^{2} sand influxes will occur. This mechanical properties log method works about 81 percent of the time (Osisanya, 2010) which is also dependent on regional environment. The one parameter method is practical but conservative.

The two parameter methods require the depletion of the reservoir pressure (ΔP_{de}) and the drawdown pressure (ΔP_{dd}) which were not considered in the one-parameter model. Stein et al., (1972) provided a technique to evaluate the maximum sand-free rate production from density and acoustic velocity log data by relating drawdown to the dynamic shear modulus, E_s. Data from wells producing sand were used to correlate to new wells.

$$(P_R - P_W)_C \propto E_s \ldots \ldots \ldots 2.19$$

$$[(P_{\mathrm{R}} - P_w)_C]_Z = [(P_R - P_W)_C]_T \left[\frac{(E_S)_z}{(E_S)_T}\right] \ldots\ldots\ldots\ldots\ldots\ldots\ldots\ldots\ldots\ldots\ldots\ldots\ldots 2.20$$

Veeken et al., (1991) plotted the total drawdown pressure, ($\Delta P_{td} = \Delta P_{de} + \Delta P_{dd}$) versus sonic transit time, Δt_c, using data from many fields of sand and non- sand producing wells. From the plot shown in Figure 2.12, a risk region possible to produce sand was established. To the left of the region, sand-free production can be expected. It was also inferred that increasing total drawdown increases the risk of sand production. The position of the risk region is field or region dependent and its can be determined from sand production tests or routine checks.

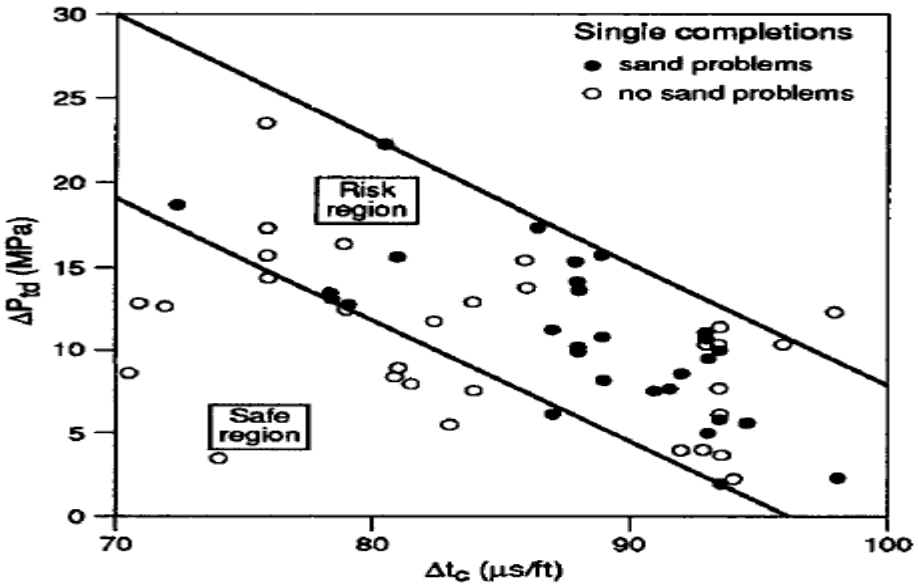

Figure 2.9: Total drawdown versus transit time for intervals with and without Sand problem (Source: Veeken et al., 1991)

To improve the resolution between sand and non-sand producers, multiple parameter correlations can be used. Fig 2.10 gives a view on how multiple-discriminant analysis techniques are used for the data set of Fig. 2.10. Sand production is related to a wide range of parameters including depth, sonic transit time, production rate, drawdown pressure, productivity index, shaliness, water-cut and gas cut. The sand and non-sand producing wells are well differentiated. The parameter influencing sand production mostly in the case of Fig.

2.9 is water-cut; sand and no sand producers are characterized by an average water-cut of 19% and 2%, respectively. The discriminant function describing the influence of the various factors is regionally/field dependent. Ghalambor et al (2002), in a similar manner, used multiple linear regressions to correlate the critical drawdown pressure observed in water-producing gas wells with seven different parameters (Veeken et al., 1991). This multi-parameter technique is limited in use because of the large number of data requirement which is not always available. Empirical techniques have the advantage of being directly related to field data and can utilize easily measurable parameters to provide routine and readily practical methods to estimate sanding risk on a well by well basis. However, revalidation and recalibration of the empirical method is needed with data from the new environment when transferred from field to field. This revalidation process requires large data acquisition for the new field that may involve field tests and laboratory measurements (Qui et al, 2006).

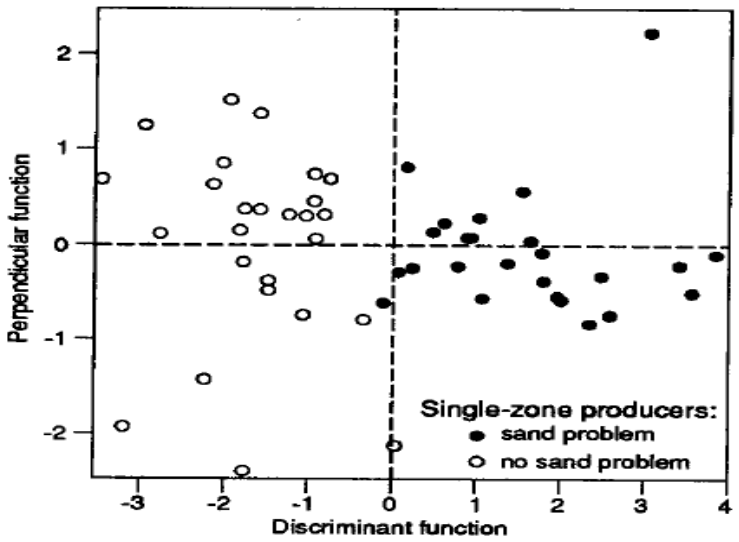

Figure 2.10: Plot Showing Result of Multiple-discriminant Analysis (Source: Veeken et al., 1991)

2.4.3.2 Laboratory Simulation

This method is used widely to establish a correlation between the risk of sanding and measurable parameters like stress, flow rate, and rock strength and to give an insight into the

mechanism of sanding in the formation involved. Laboratory experiments involve the use of available core samples or outcrop with similar mechanical properties. There are two common types: laboratory sand production experiments and hollow cylinder collapse tests (Qui et al, 2006). Laboratory experiments formulate sand production phenomenon in a controlled environment. The laboratory sand production test involves the use of cores samples to produce a small-scale simulation of flow through perforations or cylindrical cavities contained within a stressed cylindrical core sample. The method helps to the investigate factors such as drawdown, stress boundary conditions, flow rates, water cuts and rock properties. Conditions expected in the course of production from the well can be chosen as test parameters. This method is widely used to calibrate and validate predictions obtained from analytical and numerical models. However, a large number of cores and well-equipped facilities are needed for the test.

Another test used for sanding evaluation and calibration is the thick wall cylinder tests (TWC); it is easier to perform this test than sand production test. In this test, a hollow cylindrical core plug is loaded axially and laterally subject under an increasing hydrostatic stress until the sample collapses in the walls of the cylinder. The hydrostatic stress at which failure starts in the internal wall is reported as the TWC-internal and the stress that causes external wall failure is called TWC-collapse. The external wall catastrophic failure pressure corresponds to the perforation failure condition that causes continuous and catastrophic sand production. The internal wall failure pressure is less than the catastrophic failure and normally corresponds to the onset of transient sanding. TWC-internal can be defined by an increase in fluid volume expelled during constant loading or by monitoring and measuring the internal hole deformation during tests using internal gauges or camera. However, such measurements require large plug sizes which are not routinely available (Khaksar et al, 2009). For example, BP reports using plugs that have a 1.5 in outside diameter (OD), a 0.5 in. internal diameter (ID) and are 3 in. long (Willson et al., 2002), whereas Shell uses plugs that have a 1 in. OD, 0.33 in. ID and are

2 in. long (Veeken et al., 1991: Bellarby, 2009). Results from TWC test can be used to predict the depths and conditions at which sanding might occur in the field if the stresses corresponding to failure are considered representative of stresses at the sand-face or perforation cavity. Veeken et al, (1991) gave a relationship between the near-wellbore vertical effective stress ($\sigma_{v,w}$) and the TWC-collapse pressure (σ_{twc}) from many experiments carried out on friable-consolidated sandstone which is given by:

$$\sigma_{v,w} = 0.86 \times \sigma_{\text{twc}} \ldots\ldots\ldots\ldots\ldots\ldots\ldots\ldots\ldots\ldots\ldots\ldots\ldots\ldots\ldots\ldots\ldots\ldots\ldots\ldots\ldots\ldots\ldots\ldots 2.21$$

Sample size/hole size ratio of the hollow cylinder influences the results from TWC.

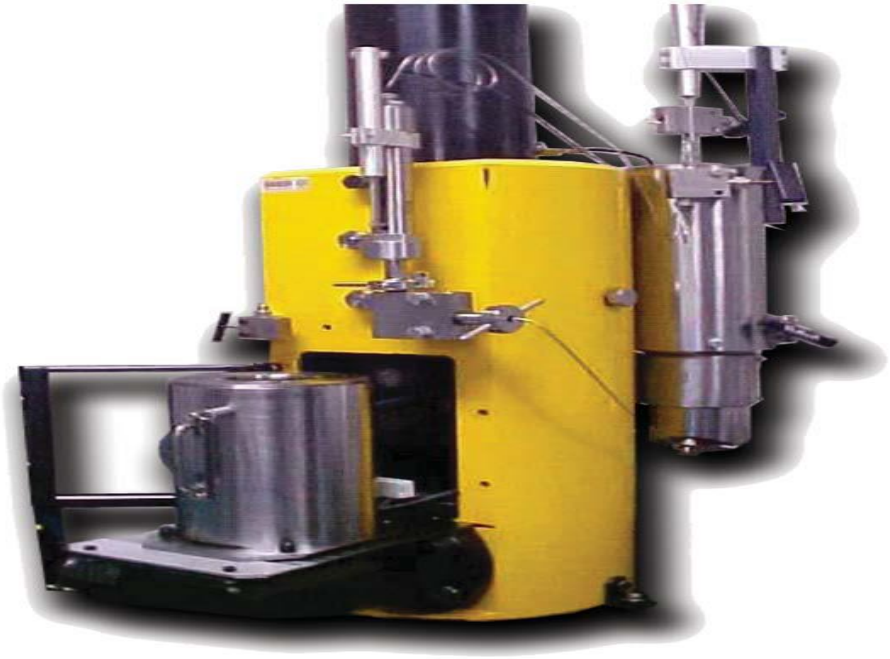

Figure 2.11: TWC Machine (Source: Bellarby, 2009)

2.4.3.3 Analytical Methods

This technique has gained more usage and popularity in the petroleum industry due to its simplicity of computation, readily implementable calculations, and running multiple realizations is easily achievable to compare many different scenarios. Analytical sand prediction models are based on modelling of perforations and production cavity stability. This tool requires a mathematical model of the sand failure mechanism. Production cavity stability under producing conditions is related to the stresses imposed on the formation matrix and the

complex manner in which the matrix accommodates these stresses. Stresses imposed are due to overburden pressure, pore pressure, flowing fluid pressure gradient near the wellbore, interfacial tension effects, and viscous drag forces. At the point of the mechanical failure of the load bearing sand grain matrix sand is assumed to be produced. Prediction accuracy depends more on how the rock constitutive behaviour is modelled, the failure criterion selected and whether the materials and other variables affecting the rock failure are determined accurately. Moore, (1994) listed some engineering and geologic parameters to be taken seriously in a complete evaluation of the sand production potential of a formation based on different sand prediction models and approaches available in the industry. However, no single sand prediction technique can accommodate all data listed below reason being that the process of data acquisition is difficult and extensive, and such information is not always available during field development.

Some of the Data required in a complete evaluation for predicting sand production potential includes:

- Field data
- Cyclic loading directional in-situ stresses
- Quality of cementation
- Perforation geometry and spacing
- Perforation cavities geometry and shot density
- Cavity evolution effect of varying perforation geometry
- Well pressure
- Flow rate
- Permeability
- Viscosity
- Relative permeability for two and three phase flow behaviour

- Rock deformation characteristics
- Rock strength characteristics
- Flow through porous media where non-Darcy flow is included
- Log-derived rock mechanical properties
- Regional tectonic forces.

2.4.3.4 Numerical Methods

Numerical models provide a detailed description of the stress state and can be accurate. They are finite element analysis models that incorporate the full details of formation behaviour during plastic, elastic and time-dependent deformation. In comparison to other methods of prediction, a numerical method is considered as more superior because it accounts for more factors influencing rock failure and sand production. However, the main drawback of the method is its complexity and time consumption. Time, resources and data needed for this method might not be available. When properties needed in the numerical modelling are assumed due to lack of real data, results from the complex modelling are not necessarily more accurate than that from other approaches that use simpler easily accessible and available data. Another method used in sand prediction is the historical method. This relies on production history such as rate, drawdown, water-cut etc. from other wells in the same reservoir or nearby fields (offset data) to arrive at a choice between sand control and sand prevention. The most critical factors to determine the sand production potential of a reservoir formation are formation strength, in-situ stresses, and production rate. Formation strength is, however, the key factor needed. Zhang et al., 2000 developed a simple and efficient approach to evaluating formation strength. They also constructed a universal failure envelope in which the only parameter needed was the critical pressure. Log data of compressional wave velocities can be used to obtain the failure envelope of a sandstone formation. The failure envelope is constructed from the critical pressure, p_c determined.

$$p_c = 10.086 \times In \frac{(6.789)}{12.322 - V_p} \ldots\ldots\ldots\ldots\ldots\ldots\ldots\ldots\ldots\ldots\ldots\ldots\ldots\ldots\ldots\ldots\ldots\ldots\ldots\ldots\ldots\ldots\ldots 2.22$$

Where,

P_c = critical pressure (psi)

V_p = compressional wave velocity (ft/s)

CHAPTER 3

3.0 METHODOLOGY

3.1 UNCONFINED COMPRESSIVE STRENGTH CORRELATION EVALUATION PROCEDURE

The methodology for UCS correlation evaluation is divided into five steps:

1) Acquisition of Log data and rock mechanics data from a field in the Niger Delta;

2) Validation of obtained data for quality check of data;

3) Statistical computations (Error analysis: relative absolute, standard deviation, correlation coefficient);

4) Graphical analysis of correlation evaluated (use of cross plot)

(5) Ranking of correlations: Sensitivity analysis to obtain acceptable parameter strength by carrying out a multiple statistical optimization of the statistical parameters.

A flow chart describing the methodology is hereby presented.

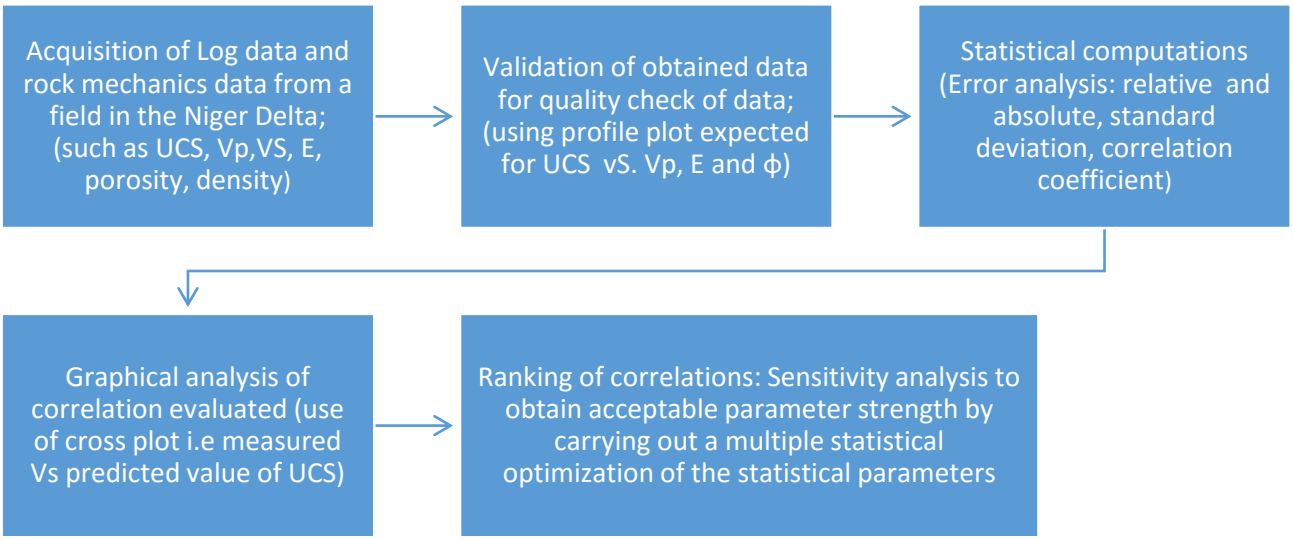

Figure 3.1: Flowchart of Procedure for Evaluating the UCS Correlations

3.1.1 Acquisition of Log Data

As part of any research, data is required for complete and proper realization of its objectives. The data used for this work were log data from well D4 in a field in the Niger Delta. The data includes porosity, density, unconfined compressive strength, compressional sonic velocity, shear sonic velocity, young modulus, tensile strength, Poisson ratio.

3.1.2 Data Validation and Quality Checking

The petrophysical and rock mechanics data used in this evaluation were validated by visual inspection to quality check the profile expected from the porosity versus depth plot; unconfined compressive strength versus porosity; p-wave velocity or interval transit time and young modulus based on theory.

3.1.3 Statistical Computations (Statistical Error Analysis)

The correlations were evaluated using five statistical measures: Average % relative error, average absolute percentage error, the standard deviation of percentage relative error, the standard deviation of percentage absolute error and correlation coefficient were computed for all the twenty-two (22) different correlations. The statistical parameters are defined as follows:

3.1.3.1 Average Percentage Relative Error (Er)

The average percentage relative error is defined as:

$$E_r = \left(\frac{1}{n}\right) \sum_{i=1}^{n} E_i \quad \text{..... (3.1)}$$

The relative deviation in percent of an estimated value from a measured value and is defined by:

$$E_i = \left[\frac{(X)_{log} - (X)_{cal}}{(X)_{log}}\right] \text{ x } 100;\ i = 1, 2 \ldots n \quad \text{..... (3.2)}$$

Where X_{log} and X_{cal} represent the unconfined compressive strength (UCS) from the geophysical log and calculated values respectively. The term Er is an indication of the relative deviation in

percent from the experimental values. The lower the value of Er the more equally distributed are the errors between positive and negative values.

3.1.3.2 Average Absolute Percentage Relative Error (Ea)

The average absolute percentage relative error is defined as:

$$E_a = \left(\frac{1}{n}\right) \sum_{i=1}^{n} |E|_i \quad \text{..... (3.3)}$$

Where E_a, indicates the relative absolute deviation in percent from the experimental values of UCS. The lower the Ea (error), the better is the correlation.

3.1.3.3 Standard Deviation

The standard deviation of the data is a reflection of the dispersion of the data around the mean. It is expressed as the square root of the variance.

$$S = \sqrt{\sum_{i=1}^{n} \left[((E_i - (\bar{X} - X_{cal})/(X_{\log})_i)\right]^2 \Big/ n-1} \quad \text{..... (3.4)}$$

The lower the value of the standard deviation, the smaller is the degree of dispersion of the data.

3.1.3.4 Correlation Coefficient

The correlation coefficient R represents the degree of success in lowering the standard deviation by regression analysis. On the other hand, the coefficient of determination is simply the square of the correlation coefficient and defined by:

$$R = \sqrt{1 - \sum_{i=1}^{n} \left[((X)_{log} - X_{cal})\right]^2 \Big/ \sum_{i=1}^{n} [(\bar{X} - X_{cal})]^2} \quad \text{..... (3.5)}$$

Where,

$$\bar{X} = \frac{1}{n}\sum_{i=1}^{n}\left[X_{log}\right] \quad \text{..... (3.6)}$$

Generally, correlation coefficient R lies between 0 and 1. A value of 1 indicates a perfect correlation whereas a value of 0 implies no correlation at all among the dependent variables and given independent variables. The larger the value of R, the greater is the reduction in the sum of square errors, and the stronger is the relationship between the independent and dependent variables.

3.1.3.5 Graphical Analysis (Use Of Cross Plots)

Graphical analysis of the evaluated correlations will be carried out using cross plots. The cross plot is a graph of the predicted versus the measured value of UCS with a 45˚ reference line to easily establish the correlation's fitness and accuracy. A perfect correlation would plot as a straight line with a slope of 45˚. The visual examination of these cross plots would give a basis for a compromise where necessary; especially where statistical results might be misleading; in cases where statistical results rank a correlation high while the cross plot clearly predicted negative values.

3.1.3.6 Ranking of Correlation (Sensitivity and Statistical Parameter Optimization)

The method which will be employed to combine all the statistical parameters into a single comparable parameter is Rank since in some cases there might be some difficulty in knowing which of the statistical parameter to rely on when making a choice of the best correlation. Hence, there is need for a new screening technique that combines all the statistical parameters into a single parameter. This technique is called Multiple Statistical Optimization Model using the Rank as a single criterion. According to Ikiensikimama et al (2008), the use of multiple combinations of statistical parameters to choose the best correlation can be represented as a constraint optimization problem with the objective function formulated as:

Min $Z_j = \sum_{j=1}^{m} S_{i,j} q_{i,j}$ ……..…… (3.7)

Subject to:

$\sum_{i=1}^{n} S_{i,j} = 1$ ……..…… (3.8)

With constraint of

$0 \leq S_{i,j} \leq 1$ …… (3.9)

Where $S_{i,j}$ is the strength of the statistical parameter j of correlation i and $q_{i,j}$ the statistical parameter j corresponding to correlation i. j = Er, Ea…..R^1, where $R^1 = 1 - R$ and Zj is the Rank (R) of the desired correlation and i is the number of correlations for a particular unconfined compressive strength (UCS).

3.1.3.7 Critical Drawdown Pressure Prediction Using UCS Method.

The ranked UCS correlations will be applied to evaluate the critical draw down pressure of the reservoir, that when exceeded, the well will draw in sand thereby causing sand production. Evaluation of critical drawdown pressure will be used to validate the two top ranked UCS correlations which will be compared against the measured reservoir critical draw down pressure.

Fjær et al. (1992) proposed the following equation for estimating the critical drawdown pressure (CDP):

CDP = n x UCS = $n \frac{2C_S Cos\emptyset}{1-Sin\emptyset}$…… (3.10)

Where UCS is the unconfined compressive strength, Cs is the cohesion, ∅ is the internal friction angle, and n is an empirical coefficient that is related to the well flow geometry. The empirical coefficient, *n*, ranges from 1 to 2 depending on whether it is an open hole (i.e., *n*=1) or a cased

hole (i.e. *n* =2). Sometimes, *n* is chosen as a variable between 1 and 2 depending on the uncertainty level of the sanding analysis.

3.2 PROCEDURE FOR SAND PRODUCTION PREDICTION

One of the applications of evaluation of UCS correlations is to predict sand production. Sand production rate will be predicted in this thesis using an easy to use mechanistic model proposed by Udebhulu and Ogbe (2015).

Sand production prediction was carried out in the following steps listed below:

Before predicting sand production rate we have to know whether the formation will produce sand or not.

3.2.1 Estimation of the two elastic constants (Bulk and Shear Modulus)

Literature theorized that sand production can be expected if the product of two elastic parameters (i.e. $G*K_b$) is lower than the threshold value of $8E11psi^2$, where the shear modulus, G and the bulk modulus, K_b are derived accurately from interpretation of acoustic and density logs (Tiab, 2014; Osisanya, 2010). Thus, it is recommended to ensure $G*K_b$ is less than $8E+11psi^2$, before even predicting the sanding rate since sand can only be produced after formation fracturing or failure has occurred.

3.2.2 Determination of Effective Formation Strength, U

Thick-walled cylinder test (TWC) is used as the fundamental strength measure for unsupported boreholes and perforations. A relationship between the effective in-situ strength of the formation, U and the TWC strength is necessary since the TWC test does not directly replicate perforation collapse pressures. This is because the standard TWC test is performed on specimens where the ratio OD/ID = 3, at in-situ conditions, the effective strength would be represented by a TWC strength where OD/ID tends to infinity. Also, there is an ID scaling

issue too, as perforation tunnels may easily exceed 0.5 inches in diameter when deep penetrating perforating charges are used in low- strength sandstones (Wilson et al, 2002).

$$U = 3.10 * TWC_{sp} \quad \ldots\ldots\ldots\ldots\ldots\ldots\ldots\ldots\ldots\ldots\ldots\ldots\ldots\ldots\ldots\ldots\ldots 3.10$$

Where,

Collapse pressure of the standard specimen TWC_{sp}, and the equivalent formation strength is U

3.2.3 Determination of loading factor (LF)

If LF < 1, the formation has not failed, while for LF > 1, the formation has failed and sand may be produced.

$$LF = \frac{3\sigma_1 - \sigma_2 - 2P_{wf} - A(P_R - P_{wf})}{3.10 * TWC} \quad \ldots\ldots\ldots\ldots\ldots\ldots\ldots\ldots\ldots\ldots\ldots\ldots 3.11$$

3.2.4 Determination of Fluid Flow Effects

The removal of shock-damaged and mechanically-weakened debris due to non-Darcy flow or turbulence in the region adjacent to the perforation cavity was correlated with the non-dimensional Reynolds number, defined by:

$$Re = 1.31735E - 12 * \frac{K\beta\rho v}{\mu} \quad \ldots\ldots\ldots\ldots\ldots\ldots\ldots\ldots\ldots\ldots\ldots\ldots\ldots\ldots\ldots\ldots\ldots 3.12$$

Where,

$$\beta = {}^{2.65E10}/_{K^{1.2}} \quad \ldots\ldots\ldots\ldots\ldots\ldots\ldots\ldots\ldots\ldots\ldots\ldots\ldots\ldots\ldots\ldots\ldots\ldots\ldots\ldots\ldots\ldots 3.13$$

Where:

K is the permeability (in mD); β is the non-Darcy flow coefficient (having dimensions of ft^{-1}); v is the velocity of the fluid crossing the lateral surface of the perforation or well (in inches/second); ρ is the density (in lb/ft^3) and μ is the viscosity (in cP).

Laboratory studies have shown a value of Re>0.1 is necessary for effective perforation clean-up during under-balance flow. Thus similar high values of Reynolds number are needed for massive sand production rates. At Reynolds numbers less than 0.1, the sanding rate is dominated by the loading factor.

3.2.5 Prediction of sand production rate using model developed by Udebhulu (2015)

In 2015, Udebhulu proposed the following relationship for predicting sand production:

$$SPR = ae^{(bW+cG)}Re^{d}LF \ldots\ldots\ldots\ldots\ldots\ldots\ldots\ldots\ldots\ldots\ldots\ldots\ldots\ldots\ldots\ldots\ldots\ldots\ldots 3.14$$

Where:

w is the water-cut in fraction; G is the gas-liquid ratio; ‘a’ has the same unit as SPR called the SPR constant of proportionality and its magnitude depends on the unit of SPR used; ‘b’, ‘c’ and “d” are the SPR correlation index, whose magnitude depends on the terrain investigated and requires real field data and experimental data obtained from core samples of the desired terrain for their determination.

The above-proposed methodology was followed strictly and the results obtained from each of the steps are presented in chapter four.

CHAPTER 4

4.0 VALIDATION OF CORRELATION, RESULT, AND DISCUSSION

4.1 VALIDATION OF THE FIELD DATA

The rock mechanics data which include unconfined compressive strength UCS, porosity, P-wave, young modulus used in this evaluation were validated using two methods: a quick visual inspection of the data and its trends, and analysis of the profiles expected from porosity versus depth plot, porosity, interval transit time, and young modulus versus unconfined compressive strength plots. The results published in the open literature was the basis for comparison (see Figure 4.1- 4.3). A total of forty-three (43) reports were gathered, forty-one (41) data points were validated for this work.

This evaluation used forty-one (41) data points. Table 4.1 shows the correlations evaluated and Table 4.2 shows the field data used for this study from an onshore well in the Niger Delta terrain. The range of input data defined by each author as well as the UCS data range considered in this study is presented in Table 4. 5.

Table 4.1: List of the UCS Correlations Evaluated

Correlation number	UCS (Mpa)	Regions where developed	General comments	Reference
(1)	0.035Vp – 31.5	Thuringia, Germany	-	Freyburg(1972)
(2)	1200exp(-0.036Δt)	Bowen basin, Australia	Fined grained, both consolidated and unconsolidated	McNally (1987)

			sandstones with all porosity ranges	
(3)	$1.4138\times10^{7}\,\Delta t^{-3}$	Gulf coast	Weak and unconsolidated sandstones	
(4)	$3.3\times10^{-20}\rho^{2}Vp^{4}[(1+v)/(1-v)]^{2}$ $(1-2v)[1+0.78V_{clay}]$	Gulf coast	Applicable to sandstones with UCS > 30 Mpa	
(5)	$1.745\times10^{-9}\ \rho V_p^{2}-21$	Cook inlet, Alaska	Coarse grain sandstone and conglomerates	Moos et al (1999)
(6)	$42.1\ \exp(1.9\times10^{-11}\rho Vp^{2})$	Australia	Consolidated sandstone with $0.05 < \emptyset < 0.12$ and UCS > 80Mpa	
(7)	$3.87\exp(1.14\times10^{-10}\ \rho V_p^{2})$	Gulf of Mexico		
(8)	46.2exp(0.027E)	-	-	-

(9)	2.28+ 4.1089E	World wide	-	Bradford et al (1998)
(10)	$254(1- 2.7\emptyset)^2$	Sedimentary basins Worldwide	Very clean, well-consolidated sandstones with $\emptyset < 0.3$	Vernik et al (1993)
(11)	$277\exp(-10\emptyset)$	-	Sandstone with 2<UCS<360Mpa and $0.002< \emptyset < 0.33$	
(12)	$2.45V_p^{1.92}$			Militzer and Stoll(1973)
(13)	$10^{0.385Vp- 0.283}$			Golubev and Rabinovich (1976)
(14)	$1277\exp(-\frac{11.2}{Vp})$			McNally(1978)
(15)	$36V_p - 31.2$			Goktan (1988)
(16)	$35.5V_p - 55$			Tugrul and Zarif(1999)
(17)	$9.95V_p^{1.21}$			Kahraman(2001)

(18)	$31.5V_p - 63.7$			Yasar and Erdrogan (2004)
(19)	$22.03V_p^{1.247}$			Sousa et al (2005)
(20)	$64.2V_p - 117.99$			Sharma and Singh (2008)
(21)	$36V_p - 45.37$			Sharma and Singh (2010)
(22)	$258e^{-9\emptyset}$		Use for porosity up to 30%. Unconfined compressive strength of the in-situ undamaged sand- Stones	Source (Tiab and Donaldson,2004)
(23)	$f(\theta_f)\frac{\rho_b^2}{\Delta t_s^2}[\Delta t_c^2 - \frac{4\Delta t_s^2}{3}]\ g(V_{sh})$		Where f=factor, ($\theta_f =$ frictional angle	Sarde et al(1993)

(24)	$0.087\times 10^{-6}EK_b[0.008V_{sh}+ 0.0054(1- V_{sh})]$		For sand strength limit, the internal friction angle $\emptyset_f = 30^\circ$	Coates and Denoo (1981) Bruce (1990)

Table 4.2: Unconfined Compressive Strength Data for Well D4

	Well D4 Data			
Unconfined compressive strength	Compressional Sonic Velocity Δtc	Shear sonic velocity Δts	Young Modulus	Tensile strength T
UCS(log) psi	(µs/ft)	(µs/ft)	E(psi)	(Psi)
1887.99	146.137	497.839	308546.3	27.48
4414.82	134.299	374.411	587565.4	76.7
3605.95	129.18	336.662	678231.4	42.97
8505.03	124.443	245.651	1309906	99.93
7103.78	134.822	301.079	887972	86.59
3989.58	131.865	337.352	676610.3	44.24
3727.21	180.095	323.691	733570.6	45.22
3572	135.501	335.28	665337.4	33.1
4180.63	125.764	305.537	806298.6	37.38
5201.43	124.07	270.571	1035789	52.29
4875.52	129.978	334.262	693100.3	46.7
5725.83	121.958	301.812	835538.3	41.11
6928.77	120.618	272.202	1035789	71.42
9220.64	117.828	257.769	693100.3	97.3
6149.96	117.366	283.035	835538.3	41.11
8874.77	119.649	270.487	1065509	127.68
5875.69	121.491	243.039	1222113	52.81
8251.01	126.172	260.505	887631.1	65.48
6618.86	120.45	253.853	1155213	49.97
8328.4	109.6	284.895	1257264	127.68
6845.34	115.221	269.143	1142038	45.71
8047.8	119.646	216.38	1158374	76.7
9961.6	107.775	246.473	1041051	101.64
10316.67	116.893	257.121	1039638	152.08
15668.02	109.533	205.538	1637445	163.62
10239.37	110.152	259.134	1336322	152.63
12870.96	106.626	222.215	1289584	96.56
11796.26	106.424	238.789	1958503	132.9
12677.61	104.187	222.054	1279921	98.06
14646.82	102.774	214.15	1608872	157.16
17164.29	105.053	193.061	1474783	135.84
15694.2	106.226	215.006	1626935	295.19
9996.7	100.125	191.1	1830852	60.37
15768.46	105.029	210,285	2145536	232.6
10917.17	103.489	180.007	1961775	73.56
14572	100.381	207.957	1977951	96.19
10417.77	102.143	178.879	1971057	65.19
10718.07	107.314	177.647	2263783	76.38
11373.16	96.264	190.775	1821500	50.48
15477.21	106.772	210.809	2213641	208.95
13738.17	104.432	193.612	1973435	95.89

Table 4.3: Some Petrophysical Data of Well D4

Petrophysical Data for Well D4		
Depth(ft)	**Density (log), g/cc**	**Porosity (log) ,fraction**
9000	2.4016	0.3459
9100	2.1862	0.3346
9200	2.1393	0.3165
9300	2.1578	0.2917
9400	2.3749	0.3143
9500	2.2903	0.2669
9600	1.952	0.3429
9700	2.2128	0.3143
9800	1.8287	0.3293
9900	2.2013	0.3256
10000	2.3371	0.3759
10100	1.9391	0.2707
10200	2.1867	0.2481
10300	2.1959	0.2699
10400	2.2324	0.2188
10500	2.2115	0.2271
10600	2.2615	0.2143
10700	2.2568	0.1827
10800	2.2211	0.1872
10900	2.2398	0.2301
11000	2.1519	0.2459
11200	-999.25	0.1851
11300	-999.25	0.0963
11400	-999.25	0.1074
11500	-999.25	0.1882

Table 4.4: Some Rock Mechanic Data of Well D4

Depth(ft)	Overburden (psi/ft)	Pore Pressure (psi/ft)	Min Horizontal Stress(psi/ft)	Max Horizontal Stress(psi/ft)	Azimuth of maxH(deg)	Well inclination(deg)	well azimuth (deg)	poissons ratio	friction angle(deg)	shale content(%)
5842.9	0.8211	0.471	0.6136	0.6636	54	17.39	140.12	0.28	25.4	0.113
5979.9	0.8321	0.4222	0.6297	0.6797	54	17.39	140.12	0.28	25.4	0.113
6059.9	0.8401	0.42575	0.6431	0.6931	54	17.39	140.12	0.28	25.4	0.113
7,200.90	0.849	0.390507	0.6811	0.7311	54	17.39	140.12	0.28	26.11	0.3765
7,270.90	0.861	0.4023	0.7245	0.7745	54	17.39	140.12	0.28	26.11	0.3765
7,344.90	0.882	0.39728	0.7431	0.7931	54	17.39	140.12	0.28	26.11	0.3765
7,483.90	0.902	0.39199	0.7461	0.7961	54	17.39	140.12	0.28	27.54	0.221
7,574.90	0.962	0.36898	0.8125	0.8625	54	17.39	140.12	0.28	27.54	0.221
7,637.90	0.981	0.38328	0.8411	0.8911	54	17.39	140.12	0.28	27.54	0.1024

Table 4.5: Data Range for the Study

Data Range for the Study			
Parameter	**Minimum**	**Maximum**	**Mean**
Bulk density, ρb (g/cc)	1.8287	2.4016	2.11515
Porosity, ø (fraction)	0.0963	0.3459	0.2211
Poisson ratio(υ)	0.25	0.28	0.265
Interval transit time, Δt (μs/ ft)	96.264	146.137	121.2005
P-wave velocity, V_p (m/s)	3166.293	2085.746	2625.852
Shear wave velocity, Vs (m/s)	612.246	1715.76	1164.004
Geophysical log UCS (psi)	1887.99	42976.96	22432.48
Shale content, Vsh (%)	0.1024	0.3765	0.23945

Figures 4.1- 4.3: show the relationship between UCS and P-wave, Young Modulus and Porosity, these plots were used for the quality check to validate the field data. Figures 4.1-4.3 followed the profile expected from results published in open literature which served as the basis of comparison. Figure 4.1 shows that there is a marked increase in UCS (strength of the rock) as compressional wave V_P increases. From Figure 4.2, it can be seen that UCS increases with increasing Young modulus (E), i.e., there is an increase in strength as E increases which is expected since E is a measure of the stiffness of the rock. The higher the stiffness of the rock, the higher the rock strength. From Figure 4.3, it can be seen that as UCS decrease with porosity i.e. the porosity of the rock increases, the rock becomes more porous and weaker.

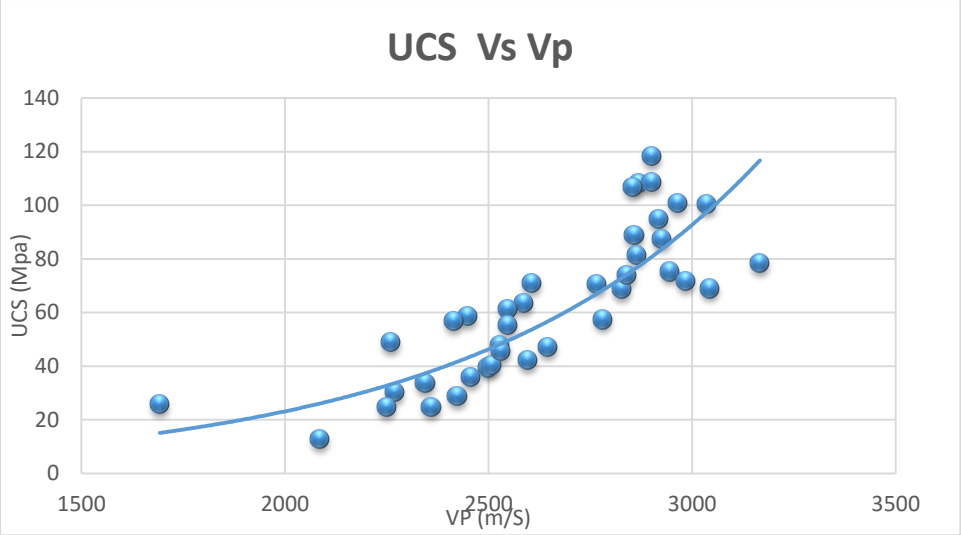

Figure 4.1: Showing plot of unconfined compressive strength vs. compressional velocity

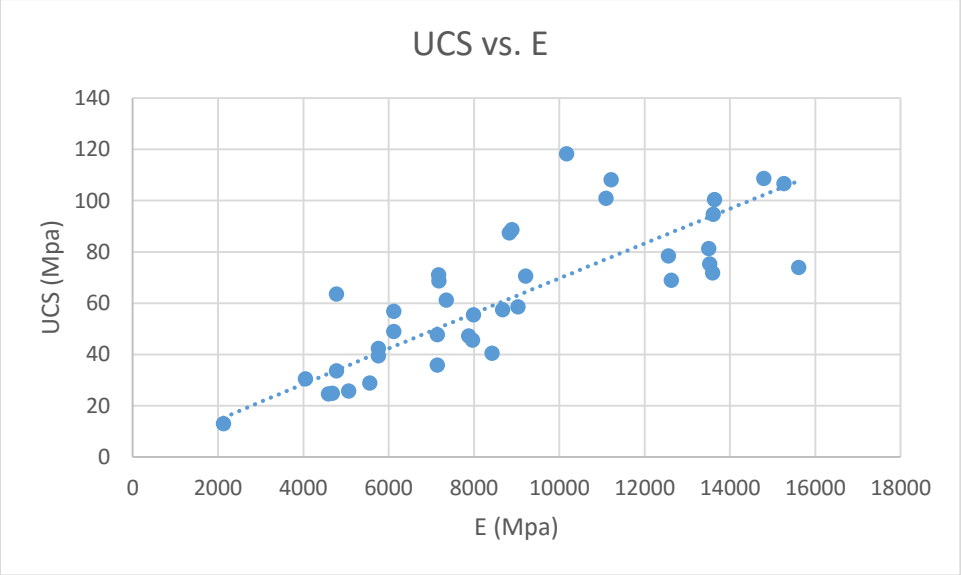

Figure 4.2: Showing Plot of Unconfined Compressive Strength vs. Young Modulus

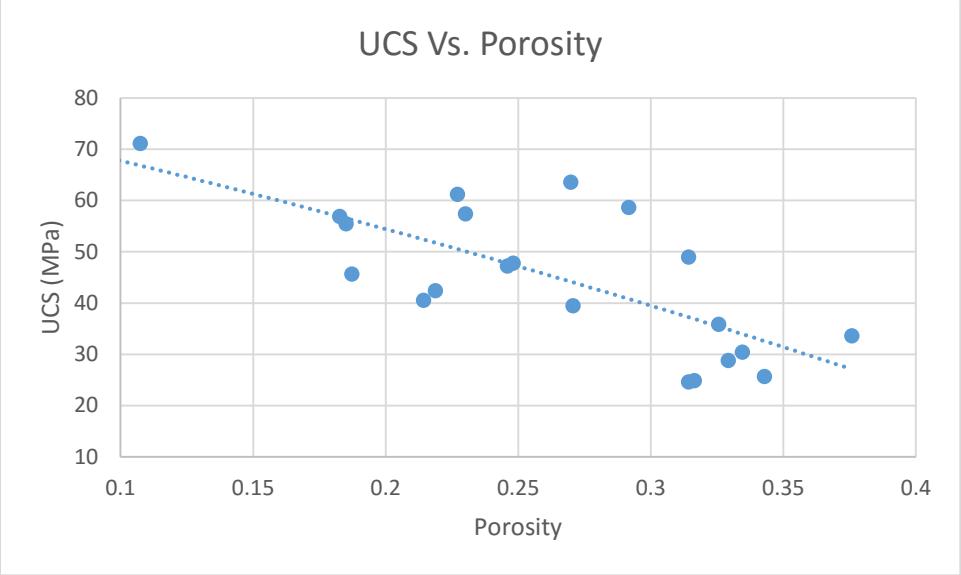

Figure 4.3: Showing plot of unconfined compressive strength vs. porosity

4.2 STATISTICAL EVALUATION

Equations 3.1-3.6 were used to evaluate the correlations in Table 4.1 to obtain the following statistical parameter (relative, absolute error: Er and Ea respectively), standard deviation (S_a and S_r), correlation coefficient R; using Dataset in Table 4.2-4.4. Table 4.6 shows the result of this calculation.

The results of the evaluation of the twenty- two of the most widely used unconfined compressive strength correlations as applied to rock strength are presented. The twenty-two (22) correlations were analysed based on the three methods stated in chapter three to choose the best correlation. From Table 4.6 it can be seen that the Sharma and Singh correlation 1.e correlation 19 that has the lowest value of absolute percentage relative error, while, Moos et al (correlation 3) has the highest value. From the statistical method, Sharma and Singh's correlation is the best. This agrees with Al-Marhoun's assertion that the best correlation should have the least absolute percentage relative error.

4.3 RANKING OF CORRELATIONS

MATLAB was used to do the sensitivity analysis and rank the correlation using the optimization model in equation (4.1- 4.3) below:

Min $Z_j = \sum_{j=1}^{m} S_{i,j} q_{i,j}$ ……..…… (4.1)

Subject to:

$\sum_{i=1}^{n} S_{i,j} = 1$ ……..…… (4.2)

With constraint of

$0 \leq S_{i,j} \leq 1$ ……... (4.3)

Table 4.6: Statistical Parameters for all the Twenty-two Correlations Evaluated

Correlations	Er	Ea	Sr	Sa	R	1-R	Rank
1	-14.1693	33.29959	52.16129	51.54443	0.97684	0.02316	54.43028
2	97.5415	97.5415	97.49543	97.49543	0.702908	0.297092	97.44448
3	-4.7E+14	4.71E+14	4.49E+15	5.48E+15	0	1	5.08E+15
4	100	100	99.93431	99.93431	0.691112	0.308888	99.89024
5	143.0018	143.0018	145.4047	145.4047	0.372965	0.627035	144.0573
6	9.625904	43.97483	58.2671	57.68769	0.93542	0.06458	51.58217
7	92.05914	92.05914	92.15449	92.15449	0.727756	0.272244	92.03903
8	-60211.2	60211.18	62071.5	63324.72	0	1	120526.3
9	99.4172	99.4172	100.1988	100.1988	0.928531	0.071469	99.79169
10	37.80581	48.1652	54.77642	54.37499	0.892622	0.107378	49.71717
11	70.59012	70.59012	71.53728	71.53728	0.828226	0.171774	71.02404
12	89.87627	89.87627	89.89513	89.89513	0.747102	0.252898	89.8227
13	68.0716	68.0716	68.49514	68.49514	0.859484	0.140516	68.24899
14	-19.8898	35.33047	56.72185	56.19467	0.977547	0.022453	62.46361
15	31.42409	34.86672	39.44737	39.20728	0.942948	0.057052	36.52675
16	38.32412	43.57386	48.45164	48.15279	0.910795	0.089205	44.98352
17	69.67199	69.67199	70.83117	70.83117	0.86126	0.13874	70.22176
18	-41.3118	50.05533	78.83488	78.75465	0.970542	0.029458	99.95903
19	13.93792	22.89906	31.89346	31.20743	0.976837	0.023163	27.10789
20	9.141407	29.32681	37.00238	36.23472	0.967113	0.032887	32.4487
21	27.73762	45.52662	53.72828	7.329958	0.910754	0.089246	43.0209
22	41.99686	45.73814	50.99189	51.02811	0.945814	0.054186	47.73087

Where:

Er = Average relative percentage error

Ea = Absolute percentage relative error

Sr = Relative standard deviation

Sa = Absolute standard deviation

R = Correlation coefficient

Figures 4.2 and 4.3 show graphically the absolute relative error and rank of the correlations evaluated.

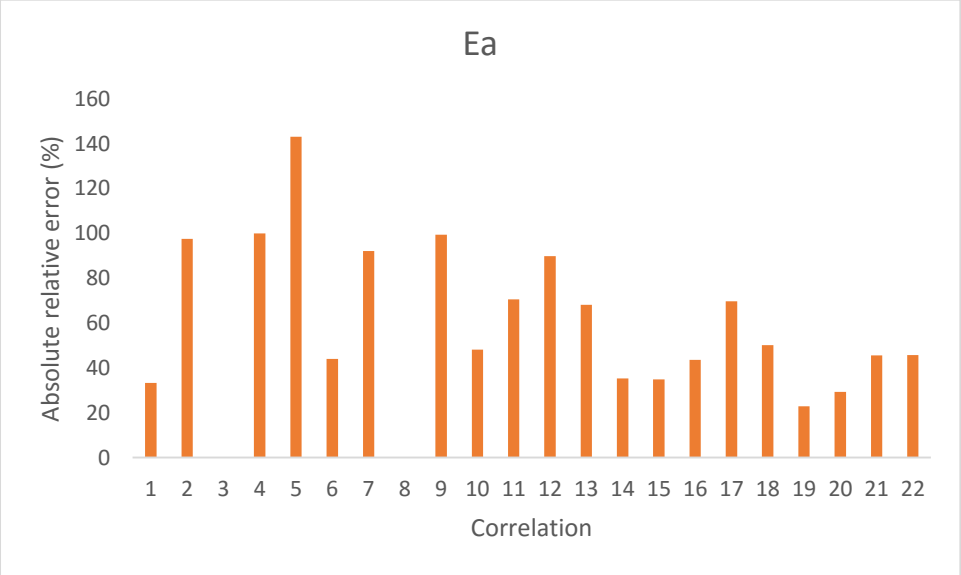

Figure 4.4: Absolute relative percentage error of evaluated correlations

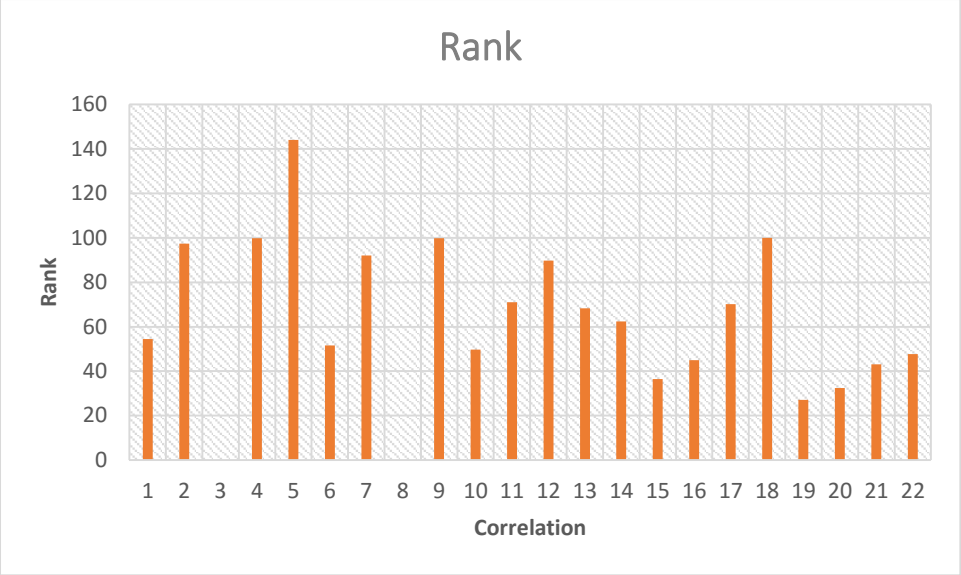

Figure 4.5: Showing Rank of evaluated correlations

The second method of choosing the best correlation combines all the statistical parameters into a single parameter called Rank for all the different correlations evaluated. Equation 4.3 was used for the ranking. From results presented in Table 4.6 it can be seen that the correlation with the lowest rank was selected as the best correlation for this geomechanical property. Sharma and Singh's correlation (1.e correlation 19) obtained the lowest value and the highest value of rank was obtained by Moos et al (correlation 3). Hence, because the best correlation should have the lowest rank (Ikiensikimama et al, 2008). Sharma and Singh (correlation 19) is also considered the best by this method. This result can also be visualised easily from Figure 4.5.

4.4 GRAPHICAL ANALYSIS OF THE EVALUATED CORRELATIONS

Cross plots of measured values of unconfined compressive strength from geophysical log against those estimated by the correlations to easily establish the correlation's fitness and accuracy of which a perfect correlation would plot as a straight line with a slope of 45˚. The visual examination of these cross plots would give a basis for a compromise where necessary; especially where statistical results might be misleading; in cases where statistical results rank

a correlation high while the cross plot clearly predicted negative values. Figure 4.6 below shows the graphical analysis of the twenty-two (22) correlations evaluated.

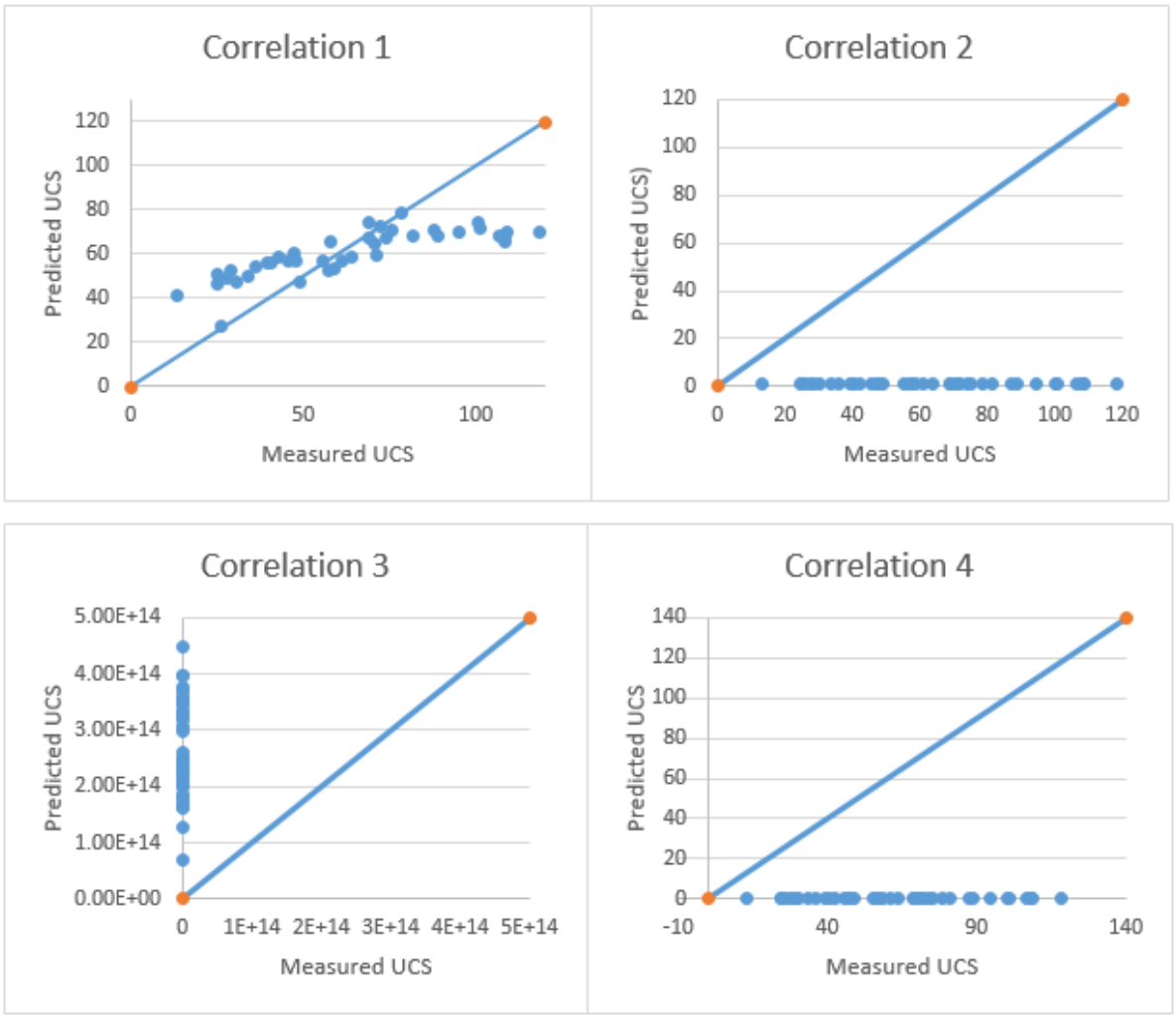

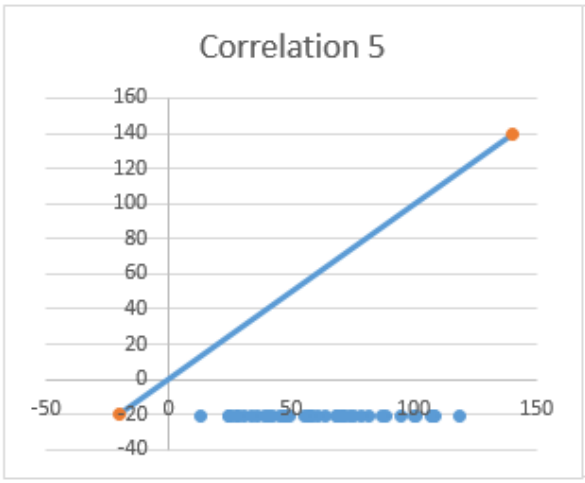
Correlation 5
160
140
120
100
80
60
40
20
0
-20
-40
-50
0
50
100
150

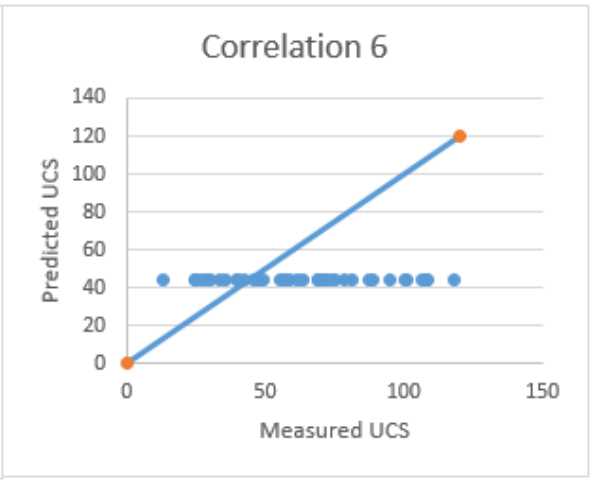
Correlation 6
Predicted UCS
140
120
100
80
60
40
20
0
0
50
100
150
Measured UCS

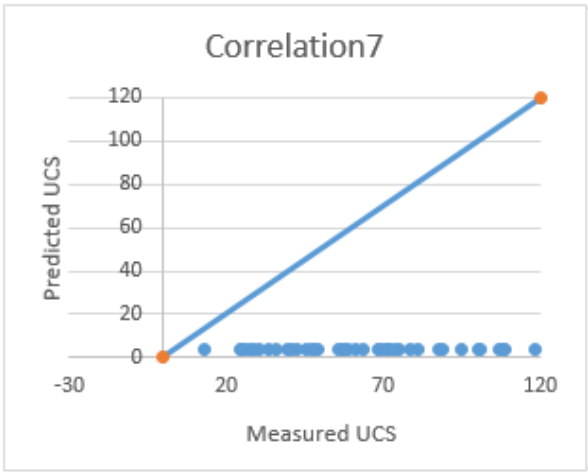
Correlation7
Predicted UCS
120
100
80
60
40
20
0
-30
20
70
120
Measured UCS

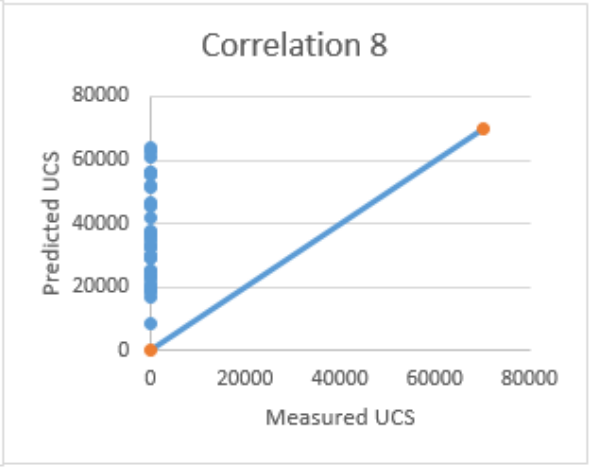
Correlation 8
Predicted UCS
80000
60000
40000
20000
0
0
20000
40000
60000
80000
Measured UCS

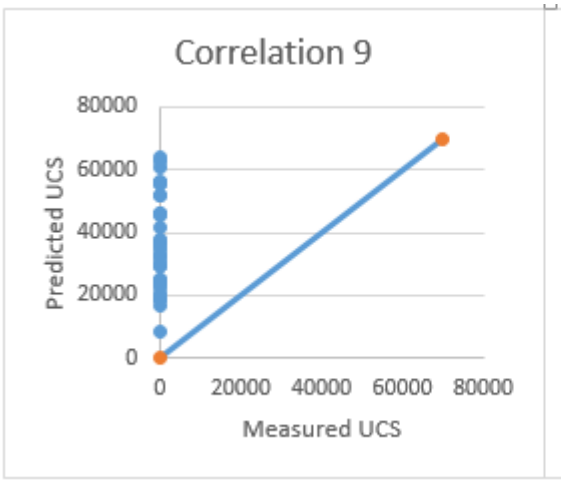
Correlation 9
Predicted UCS
80000
60000
40000
20000
0
0
20000
40000
60000
80000
Measured UCS

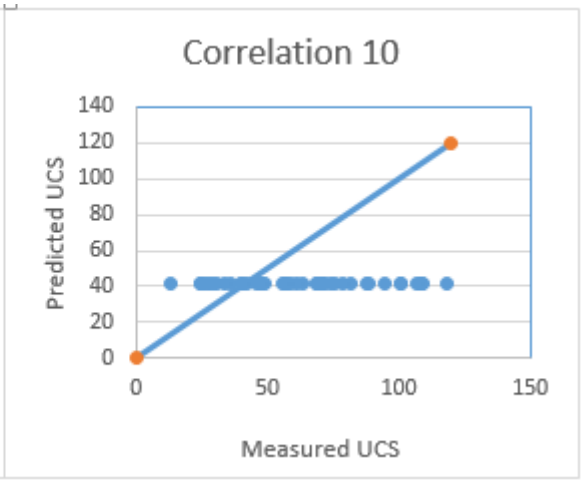
Correlation 10
Predicted UCS
140
120
100
80
60
40
20
0
0
50
100
150
Measured UCS

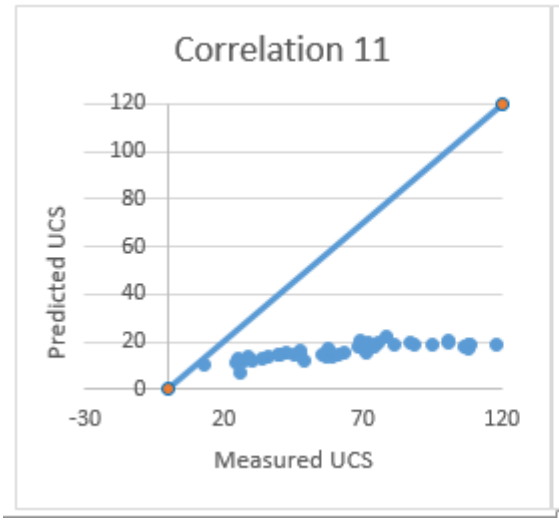
Correlation 11
Predicted UCS
Measured UCS
120
100
80
60
40
20
0
-30
20
70
120

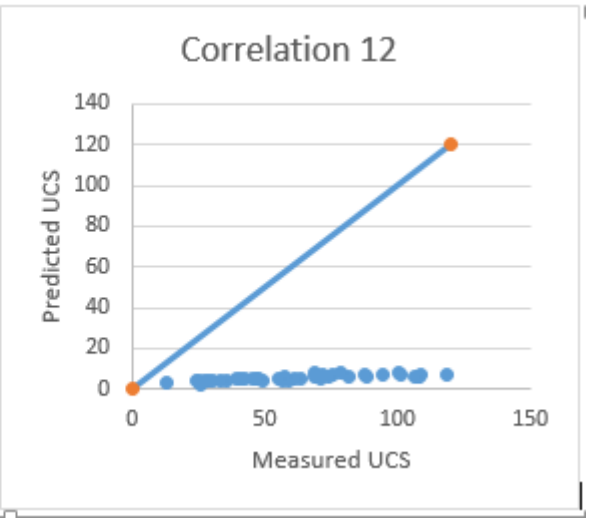
Correlation 12
Predicted UCS
Measured UCS
140
120
100
80
60
40
20
0
0
50
100
150

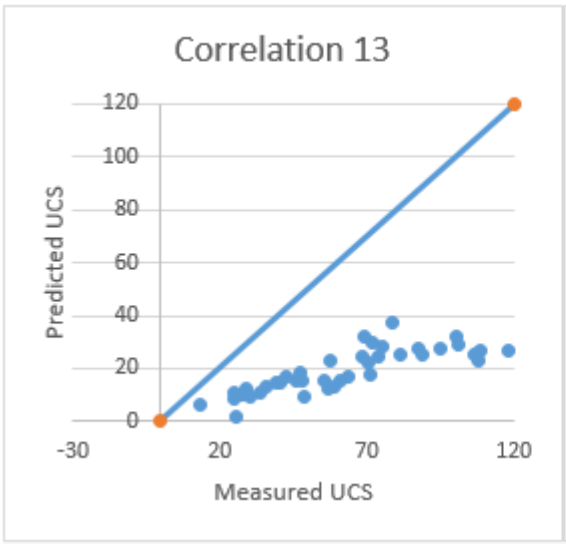
Correlation 13
Predicted UCS
Measured UCS
120
100
80
60
40
20
0
-30
20
70
120

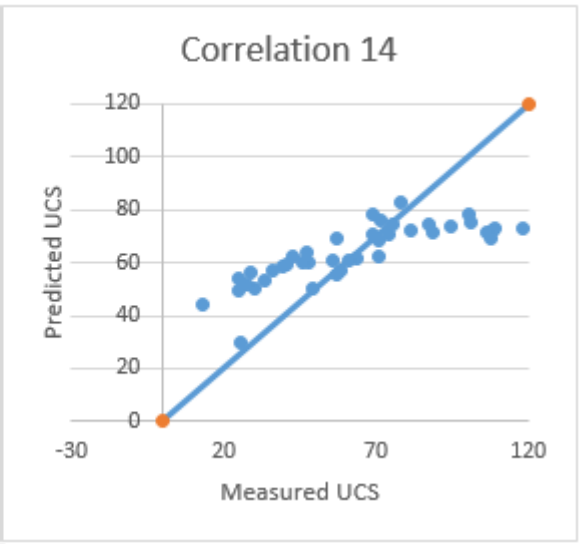
Correlation 14
Predicted UCS
Measured UCS
120
100
80
60
40
20
0
-30
20
70
120

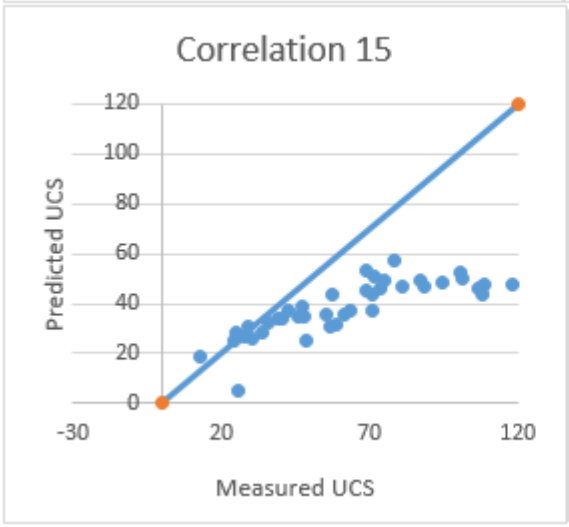
Correlation 15
Predicted UCS
Measured UCS
120
100
80
60
40
20
0
-30
20
70
120

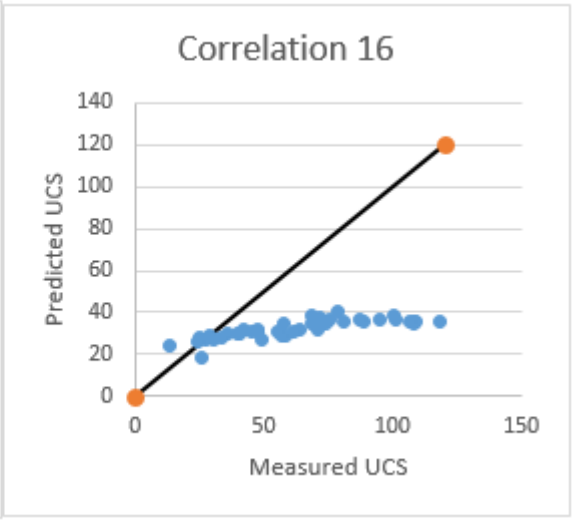
Correlation 16
Predicted UCS
Measured UCS
140
120
100
80
60
40
20
0
0
50
100
150

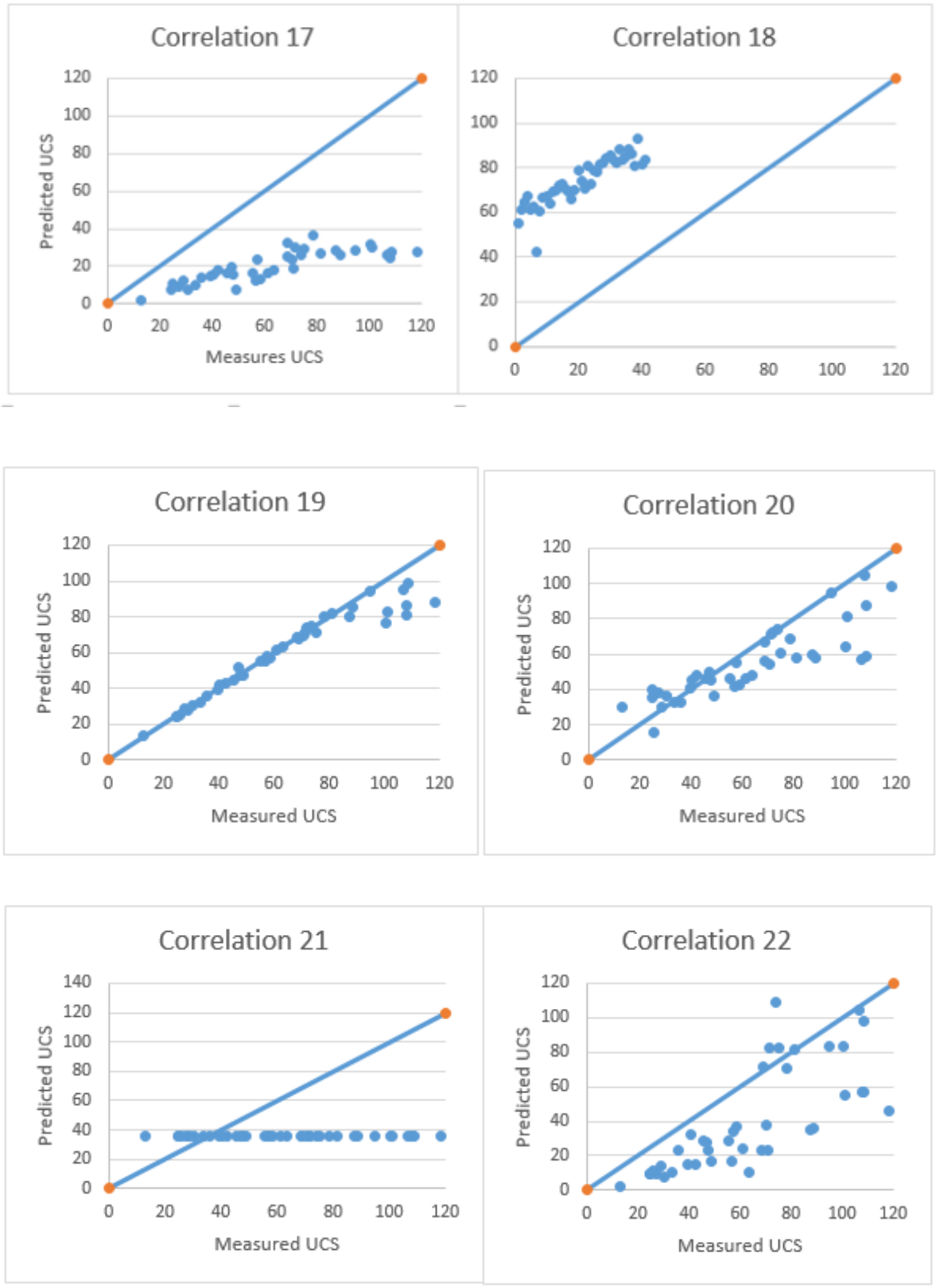

Figure 4.6: Cross Plot for the Twenty-two Correlations Evaluated

From the Figures presented in 4.6 for the twenty-two correlations evaluated. The cross plot agrees with the conclusion drawn from the statistical analysis and the Rank of the correlations. Sharma and Singh (correlation 19) gave the best cross plot which predicted correlation accuracy and fitness for UCS value of less than or equal to 75Mpa. The result is acceptable because the formation of the study is an unconsolidated sandstone terrain which is not expected to have a high rock strength of which at UCS higher than that value the formation is more strong and consolidated.

4.5 CRITICAL DRAWDOWN PRESSURE PREDICTION USING UCS METHOD.

The two best correlations evaluated using the three principal methods, i.e., statistical analysis, a method of ranking of correlation and graphical analysis, were used to estimate compressive strength from available Niger Delta data. The estimated unconfined compressive strength will be used to determine the critical drawdown pressure for formation failure and by extension sanding of the well. The two best correlation are correlation 19 and 20, (Singh and Sharma 2008 and 2010 respectively). The critical drawdown pressure was evaluated using equation 3.10.

Using cased hole condition i.e. n = 2, the weak spots of the reservoir by evaluating the UCS at various depth. The weakest spot was the sandstone interval of 6700ft using equation 4.4 to evaluate the CDP. Table 4.7 below shows the results obtained.

Table 4.7: Critical Drawn down Pressure of the two best Evaluated Correlation

Correlations	**Unconfined Compressive Strength UCS (Mpa)**			**Empirical constant (n)**	**Initial reservoir pressure (psi)**	**Critical drawdown pressure (CDP), (Mpa)**
	Min.	**Max.**	**Average**			
19	13.92	98.32	59.37	2	4664	27.84
20	20.56	109.8	50.32	2	4664	41.12
Measured	13.01	118.34	63.22	2	4664	26.02

From the results presented in Table 4.7, correlation 20 over predicted the critical drawn down pressure CDP for sand production which is too conservative when compared to the measured CDP of the well. Whereas correlation 19 compares favourably with about 7% deviation from measured CDP.

4.6 SAND PRODUCTION PREDICTION

The methodology stated in chapter three will be followed and validated by using real field data of sand production in some Niger Delta wells to determine the associated SPR correlation index which is expected to be a unique fingerprint of each well investigated.

4.6.1 Field Data of Some Onshore Niger Delta Wells

Table 4.8: Rock Mechanics Data of Well G-15

Depth(ft)	Overburden (psi/ft)	Pore Pressure (psi/ft)	Min Horizontal Stress(psi/ft)	Max Horizontal Stress(psi/ft)	poisson ratio	youngs modulus(Mpsi)	friction angle(deg)	shale content(%)
4000	0.822	0.435	0.78	0.83	0.25	0.2234	26.77	0.321
5243	0.841	0.435	0.78	0.83	0.25	0.2234	26.77	0.321
7681	0.848	0.435	0.78	0.83	0.25	0.2234	28.31	0.321
8354	0.857	0.435	0.78	0.83	0.25	0.334	28.34	0.23
9159	0.857	0.436	0.78	0.83	0.25	0.334	28.34	0.112
9714	0.871	0.439	0.79	0.84	0.25	0.334	30	0.112
10080	0.871	0.439	0.86	0.91	0.25	0.351	30	0.354
10232	0.881	0.439	0.86	0.91	0.25	0.467	30	0.354
10863	0.896	0.439	0.89	0.94	0.25	0.584	30	0.354
11414	0.923	0.415	0.89	0.94	0.25	0.547	26.5	0.543
11995	0.928	0.47	0.89	0.94	0.25	0.598	26.89	0.573
12291	0.928	0.47	0.89	0.94	0.25	0.683	26.89	0.573
12544	0.928	0.477	0.89	0.94	0.25	0.683	27.13	0.67
13214	0.928	0.465	0.89	0.94	0.25	0.683	27.13	0.443
13691	0.928	0.466	0.89	0.94	0.25	0.683	27.13	0.6891
14075	0.928	0.466	0.89	0.94	0.25	0.683	27.13	0.6891
14200	0.928	0.464	0.89	0.94	0.25	0.683	27.89	0.6891

Table 4.9: Rock Mechanics Data of Well G-14

Depth(ft)	Overburden (psi/ft)	Pore Pressure (psi/ft)	Min Horizontal Stress(psi/ft)	Max Horizontal Stress(psi/ft)	poissons ratio	youngs modulus(Mpsi)	friction angle(deg)	shale content(%)
4264	0.822	0.439	0.78	0.83	0.25	0.2234	26.77	0.321
5243	0.841	0.439	0.78	0.83	0.25	0.2234	26.77	0.321
7681	0.848	0.439	0.78	0.83	0.25	0.2234	28.31	0.321
8119	0.857	0.439	0.78	0.83	0.25	0.334	28.34	0.23
9159	0.857	0.415	0.78	0.83	0.25	0.334	28.34	0.112
9714	0.871	0.47	0.79	0.84	0.25	0.334	30	0.112
10080	0.871	0.47	0.88	0.93	0.25	0.351	30	0.354
10232	0.881	0.47	0.88	0.93	0.25	0.467	30	0.354
10863	0.896	0.465	0.89	0.94	0.25	0.584	30	0.354
11414	0.923	0.466	0.89	0.94	0.25	0.547	26.5	0.543
11995	0.928	0.466	0.89	0.94	0.25	0.598	26.89	0.573
12291	0.928	0.464	0.89	0.94	0.25	0.683	26.89	0.573
13456	0.928	0.464	0.89	0.94	0.25	0.683	26.89	0.573
14002	0.928	0.464	0.89	0.94	0.25	0.683	26.89	0.573
14076	0.928	0.464	0.89	0.94	0.25	0.683	26.89	0.573

Table 4.10: Extraction from Production Data of Well G-14

UniqueId	Date	Date	Sand	Oil	Water	Gas	Bean	THP
		Days	PPTB	bbl/m	bbl/m	Mscf/m		psi
G14	01/05/2004	26	3	9188	4313	8183	44	495
G14	01/05/2005	26	2	6400	4598	12834	44	395
G14	01/08/2005	30	2	3830	2947	24332	44	396
G14	01/11/2005	30	7	2536	1115	37364	44	361
G14	01/01/2006	28	2	8500	10625	2820	44	392
G14	01/03/2006	27	3	9952	8133	3512	44	495
G14	01/04/2006	30	4	15200	14277	3657	44	495
G14	01/05/2006	17	5	14062	7029	9472	44	495

Table 4.11: Extraction from Production Data of Well G-15

UniqueId	Date	Date	Sand	Oil	Water	Gas	Bean	THP
		Days	PPTB	bbl/m	bbl/m	Mscf/m		psi
G15	01/09/2006	29	39	14091.040	35321.620	5818.629	64	384
G15	01/06/2006	30	34	18137.390	13032.260	83393.244	64	426
G15	01/04/2007	30	32	17323.290	12686.080	2999.026	64	375
G15	01/03/2007	29	32	15850.320	11520.090	19275.441	64	435
G15	01/11/2006	30	32.5	19987.840	13790.220	15550.130	64	435
G15	01/10/2006	27	32.5	19149.970	13506.970	16623.504	60	378
G15	01/11/2006	26	34	18614.700	14326.770	5912.723	60	378

4.6.2 Determination of Sanding Potential of the Investigated Well

As proposed by Osisanya (2010) and Tiab (2014), sand production can be expected if the product of shear and bulk modulus (i.e. $G*K_b$) is lower than the threshold value of 8.0E11psi^2. The estimated sanding potential of both wells based on petrophysical properties is presented in Table 4.12 and Table 4.13.

Table 4.12: Sanding Potential of Well G-15

Depth(ft)	Poissons ratio	Youngs modulus(Mpsi)	Shear modulus G(Mpsi)	Bulk modulus Kb(Mpsi)	GKb (psi^2)	Bulk Compressibilty (1/psi)
4000	0.25	0.2234	0.08936	0.148933	1.33E+10	6.71441E-06
5243	0.25	0.2234	0.08936	0.148933	1.33E+10	6.71441E-06
7681.4	0.25	0.2234	0.08936	0.148933	1.33E+10	6.71441E-06
8,354.00	0.25	0.334	0.1336	0.222667	2.97E+10	4.49102E-06
9,159.00	0.25	0.334	0.1336	0.222667	2.97E+10	4.49102E-06
9,714.00	0.25	0.334	0.1336	0.222667	2.97E+10	4.49102E-06
10,080.00	0.25	0.351	0.1404	0.234	3.29E+10	4.2735E-06
10,232.00	0.25	0.467	0.1868	0.311333	5.82E+10	3.21199E-06
10,863.00	0.25	0.584	0.2336	0.389333	9.09E+10	2.56849E-06
11,414.00	0.25	0.547	0.2188	0.364667	7.98E+10	2.74223E-06
11,995.00	0.25	0.598	0.2392	0.398667	9.54E+10	2.50836E-06
12,291.00	0.25	0.601	0.2404	0.400667	9.63E+10	2.49584E-06
12,544.00	0.25	0.601	0.2404	0.400667	9.63E+10	2.49584E-06
13,214.00	0.25	0.601	0.2404	0.400667	9.63E+10	2.49584E-06
13,691.00	0.25	0.601	0.2404	0.400667	9.63E+10	2.49584E-06
14,075.00	0.25	0.456	0.1824	0.304	5.54E+10	3.28947E-06
14,200.00	0.25	0.456	0.1824	0.304	5.54E+10	3.28947E-06

Table 4.13: Sanding Potential of Well G-14

Depth(ft)	Poissons ratio	Youngs modulus(Mpsi)	Shear modulus G(Mpsi)	Bulk modulus Kb(Mpsi)	GKb (psi^2)	Bulk Compressibilty (1/psi)
4264.45	0.25	0.2234	0.08936	0.148933	1.33E+10	6.714E-06
5243	0.25	0.2234	0.08936	0.148933	1.33E+10	6.714E-06
7681.4	0.25	0.2234	0.08936	0.148933	1.99E+10	6.714E-06
8,118.70	0.25	0.334	0.1336	0.222667	2.97E+10	4.491E-06
9,159.00	0.25	0.334	0.1336	0.222667	2.97E+10	4.491E-06
9,714.00	0.25	0.334	0.1336	0.222667	3.13E+10	4.491E-06
10,080.00	0.25	0.351	0.1404	0.234	4.37E+10	4.274E-06
10,232.00	0.25	0.467	0.1868	0.311333	7.27E+10	3.212E-06
10,863.00	0.25	0.584	0.2336	0.389333	8.52E+10	2.568E-06
11,414.00	0.25	0.547	0.2188	0.364667	8.72E+10	2.742E-06
11,995.00	0.25	0.598	0.2392	0.398667	9.58E+10	2.508E-06
12,291.00	0.25	0.601	0.2404	0.400667	9.63E+10	2.496E-06
13,456.30	0.25	0.601	0.2404	0.400667	7.31E+10	2.496E-06
14,002.00	0.25	0.456	0.1824	0.304	5.54E+10	3.289E-06
14,076.00	0.25	0.456	0.1824	0.304	5.54E+10	3.289E-06

From Table 4.12 and 4.13 it can been seen that, the product of the shear modulus and the bulk modulus of the formations investigated in both cases for all depth considered is less than the lower limit value of 8.0E11psi^2; this suggests the possibility of formation failure in the production life of the reservoir and thus sanding when the critical drawdown pressure and flow rate required for fluidizing the loosed formation is reached. Now the results of the study will be applied to estimate the sand production conditions in the two Niger Delta wells.

4.6.3 Determination of the Formation Strength, U of the Investigated Wells

Typically for unconsolidated formation, the formation strength is determined from the TWC test in the laboratory, due to unavailability of relevant data, the formation strength will be obtained from the average of the fracture gradient of the pay-zone of the formation determined using the Ben Eaton's correlation for fracture gradient. Results of estimated formation strength are shown in Table 4.13 and Table 4.14.

$$F = \left(\frac{S-P}{D}\right)\left(\frac{\Upsilon}{1-\Upsilon}\right) + \frac{P}{D} \quad \ldots\ldots 4.4$$

Where:

F is the fracture gradient at the true vertical depth of interest.

S is the overburden pressure at the true vertical depth of interest.

P is the pore pressure of the formation (reservoir pressure) at the true vertical depth of interest.

D is the true vertical depth of interest.

Υ is the Poisson's ratio

Table 4.14: Formation Strength of Well G-14

Depth(ft)	Poissons ratio	Overburden(psi/ft)	Pore Pressure (psi/ft)	Min Horizontal Stress (psi/ft)	Max Horizontal Stress (psi/ft)	Reservoir Pressure (psi)	Fracture gradient (psi/ft)	Formation strength (psi)
4264.45	0.25	0.822	0.439	0.78	0.83	1872.094	0.5667	2416.522
5243.00	0.25	0.841	0.439	0.78	0.83	2301.677	0.5730	3004.239
7681.40	0.25	0.848	0.439	0.78	0.83	3372.135	0.5753	4419.365
8118.70	0.25	0.857	0.439	0.78	0.83	3564.109	0.5783	4695.315
9159.00	0.25	0.857	0.415	0.78	0.83	3800.985	0.5623	5150.411
9714.00	0.25	0.871	0.47	0.79	0.84	4565.580	0.6037	5864.018
10080.00	0.25	0.871	0.47	0.88	0.93	4737.600	0.6037	6084.960
10232.00	0.25	0.881	0.47	0.88	0.93	4809.040	0.6070	6210.824
10863.00	0.25	0.896	0.465	0.89	0.94	5051.295	0.6087	6611.946
11414.00	0.25	0.923	0.466	0.89	0.94	5318.924	0.6183	7057.657
11995.00	0.25	0.928	0.466	0.89	0.94	5589.670	0.6200	7436.900
12291.00	0.25	0.928	0.464	0.89	0.94	5703.024	0.6187	7604.032
13456.30	0.25	0.928	0.464	0.89	0.94	6243.723	0.6187	8324.964
14002.00	0.25	0.928	0.464	0.89	0.94	6496.928	0.6187	8662.571
14076.00	0.25	0.928	0.464	0.89	0.94	6531.264	0.6187	8708.352

Table 4.15: Formation Strength for Well G-15

Depth(ft)	Poissons ratio	Overburden (psi/ft)	Pore Pressure (psi/ft)	Min Horizontal Stress(psi/ft)	Max Horizontal Stress (psi/ft)	Reservoir Pressure (psi)	Fracture gradient (Psi/ft)	Formation strength (psi)
4000	0.25	0.822	0.435	0.78	0.83	1740.00	0.564	2256.000
5243	0.25	0.841	0.435	0.78	0.83	2280.71	0.570	2990.258
7681.4	0.25	0.848	0.435	0.78	0.83	3341.41	0.573	4398.882
8,354.00	0.25	0.857	0.435	0.78	0.83	3633.99	0.576	4809.119
9,159.00	0.25	0.857	0.436	0.78	0.83	3993.32	0.576	5278.637
9,714.00	0.25	0.871	0.439	0.79	0.84	4264.45	0.583	5663.262
10,080.00	0.25	0.871	0.439	0.86	0.91	4425.12	0.583	5876.640
10,232.00	0.25	0.881	0.439	0.86	0.91	4491.85	0.586	5999.363
10,863.00	0.25	0.896	0.439	0.89	0.94	4768.86	0.591	6423.654
11,414.00	0.25	0.923	0.415	0.89	0.94	4736.81	0.584	6669.581
11,995.00	0.25	0.928	0.47	0.89	0.94	5637.65	0.623	7468.887
12,291.00	0.25	0.928	0.47	0.89	0.94	5776.77	0.623	7653.196
12,544.00	0.25	0.928	0.477	0.89	0.94	5983.49	0.627	7869.269
13,214.00	0.25	0.928	0.465	0.89	0.94	6144.51	0.619	8183.871
13,691.00	0.25	0.928	0.466	0.89	0.94	6380.01	0.620	8488.420
14,075.00	0.25	0.928	0.466	0.89	0.94	6558.95	0.620	8726.500
14,200.00	0.25	0.928	0.464	0.89	0.94	6588.80	0.619	8785.067

4.6.4 Determination of Loading Factor of the Investigated Wells

The relationship for the loading factor (equation 3.13 and 3.14) will be used in its determination. The required Poroelastic constant is firstly determined using equation 3.5 and substituted into equation 3.14 to obtain the loading factor.

Recall:

$$C_b = \frac{1}{K_b} = \frac{3(1-2v)}{E} \ldots\ldots\ldots\ldots\ldots\ldots\ldots\ldots\ldots\ldots\ldots\ldots\ldots\ldots\ldots 4.4$$

Where: C_b is the rock bulk Compressibility.

The estimated loading factor of both wells are shown in Table 4.15 and Table 4.16

Table 4.16: Loading Factor of Well G-14

Depth(ft)	Poissons ratio	Overburden(psi/ft)	Pore Pressure (psi/ft)	Min Horizontal Stress (psi/ft)	Max Horizontal Stress (psi/ft)	Reservoir Pressure (psi)	Fracture gradient (psi/ft)	Formation strength (psi)	Poroelastic contant (A)	Loading factor (LF)
4264.45	0.25	0.822	0.439	0.78	0.83	1872.094	0.5667	2416.522	0.428	1.573
5243.00	0.25	0.841	0.439	0.78	0.83	2301.677	0.5730	3004.239	0.428	1.795
7681.40	0.25	0.848	0.439	0.78	0.83	3372.135	0.5753	4419.365	0.428	2.119
8118.70	0.25	0.857	0.439	0.78	0.83	3564.109	0.5783	4695.315	0.310	2.135
9159.00	0.25	0.857	0.415	0.78	0.83	3800.985	0.5623	5150.411	0.310	2.285
9714.00	0.25	0.871	0.47	0.79	0.84	4565.580	0.6037	5864.018	0.310	2.183
10080.00	0.25	0.871	0.47	0.88	0.93	4737.600	0.6037	6084.960	0.292	2.503
10232.00	0.25	0.881	0.47	0.88	0.93	4809.040	0.6070	6210.824	0.169	2.500
10863.00	0.25	0.896	0.465	0.89	0.94	5051.295	0.6087	6611.946	0.044	2.564
11414.00	0.25	0.923	0.466	0.89	0.94	5318.924	0.6183	7057.657	0.083	2.552
11995.00	0.25	0.928	0.466	0.89	0.94	5589.670	0.6200	7436.900	0.029	2.573
12291.00	0.25	0.928	0.464	0.89	0.94	5703.024	0.6187	7604.032	0.026	2.591
13456.30	0.25	0.928	0.464	0.89	0.94	6243.723	0.6187	8324.964	0.026	2.636
14002.00	0.25	0.928	0.464	0.89	0.94	6496.928	0.6187	8662.571	0.180	2.637
14076.00	0.25	0.928	0.464	0.89	0.94	6531.264	0.6187	8708.352	0.180	2.639
										2.352

Table 4.17: Loading Factor of Well G-15

Depth(ft)	Poissons ratio	Overburden (psi/ft)	Pore Pressure (psi/ft)	Min Horizontal Stress(psi/ft)	Max Horizontal Stress (psi/ft)	Reservoir Pressure (psi)	Fracture gradient (Psi/ft)	Formation strength (psi)	poroelastic constant A	Loading Factor (LF)
4000	0.25	0.822	0.435	0.78	0.83	1740.00	0.564	2256.000	0.42837	1.367
5243	0.25	0.841	0.435	0.78	0.83	2280.71	0.570	2990.258	0.42837	1.572
7681.4	0.25	0.848	0.435	0.78	0.83	3341.41	0.573	4398.882	0.42837	1.790
8,354.00	0.25	0.857	0.435	0.78	0.83	3633.99	0.576	4809.119	0.31040	1.819
9,159.00	0.25	0.857	0.436	0.78	0.83	3993.32	0.576	5278.637	0.31040	1.854
9,714.00	0.25	0.871	0.439	0.79	0.84	4264.45	0.583	5663.262	0.31040	1.885
10,080.00	0.25	0.871	0.439	0.86	0.91	4425.12	0.583	5876.640	0.29227	2.137
10,232.00	0.25	0.881	0.439	0.86	0.91	4491.85	0.586	5999.363	0.16853	2.130
10,863.00	0.25	0.896	0.439	0.89	0.94	4768.86	0.591	6423.654	0.04373	2.233
11,414.00	0.25	0.923	0.415	0.89	0.94	4736.81	0.584	6669.581	0.08320	2.315
11,995.00	0.25	0.928	0.47	0.89	0.94	5637.65	0.623	7468.887	0.02880	2.103
12,291.00	0.25	0.928	0.47	0.89	0.94	5776.77	0.623	7653.196	0.02560	2.110
12,544.00	0.25	0.928	0.477	0.89	0.94	5983.49	0.627	7869.269	0.02560	2.089
13,214.00	0.25	0.928	0.465	0.89	0.94	6144.51	0.619	8183.871	0.02560	2.148
13,691.00	0.25	0.928	0.466	0.89	0.94	6380.01	0.620	8488.420	0.02560	2.153
14,075.00	0.25	0.928	0.466	0.89	0.94	6558.95	0.620	8726.500	0.02560	2.160
14,200.00	0.25	0.928	0.464	0.89	0.94	6588.80	0.619	8785.067	0.02560	2.170
									Average =	2.002

From Table 4.16 and 4.17 it can be seen that values of loading factor for both wells at all depths are greater than 1 which confirms that the formation has the potential of sanding.

It is ascertained by Wilson et al (2002) that for LF < 1, the formation has not failed, while for LF > 1, the formation has failed and sand may be produced.

Table 4.18: Some Required Field Information of all Wells Investigated

Average permeability	**500Md**
Average Oil Density	53.03 lb/ft^3
Average Oil viscosity	0.8Cp
Wellbore Diameter @600ft	17-1/2''
Wellbore Diameter @4227.5ft	12-1/4''
Wellbore Diameter @8500ft	8-1/2''
Perforation Diameter	4-5/8''
Perforation average Cross- sectional Area	16.8"
Perforation Density	4 SPF
Perforation Interval	80ft
Total number of perforation	320 shots

$$Re = 1.31735E-12 * \frac{K\beta\rho v}{\mu} \ldots\ldots\ldots\ldots\ldots\ldots\ldots\ldots\ldots\ldots\ldots\ldots\ldots\ldots\ldots\ldots 3.12$$

$$\beta = {}^{2.65E10}/_{K^{1.2}} \ldots\ldots\ldots\ldots\ldots\ldots\ldots\ldots\ldots\ldots\ldots\ldots\ldots\ldots\ldots\ldots\ldots\ldots\ldots\ldots 3.13$$

$$q = nAv \ldots\ldots\ldots\ldots\ldots\ldots\ldots\ldots\ldots\ldots\ldots\ldots\ldots\ldots\ldots\ldots\ldots\ldots\ldots\ldots 4.5$$

n is the total number of the perforations while A is the average cross-sectional area of each perforation, (for simplicity, we assume half of the perforations to be effective).

Where: q is in in^3/sec.; Recall: 1bbl/month = 3.743E-03in^3/sec

The estimated Reynolds's number of both wells are shown in Table 4.15 and Table 4.16.

4.6.5 Prediction of Sand Production Rate

Sand production rate will be predicted using Udebhulu's model (2015) given by equation 3.14

$$SPR = ae^{(bW+cG)}Re^{d}LF \ \ldots\ldots\ldots\ldots\ldots\ldots\ldots\ldots\ldots\ldots\ldots\ldots\ldots\ldots\ldots\ldots\ldots\ldots\ldots\ldots 3.14$$

Linearization of the model by taking the logarithm of both sides aids the determination of the associated SPR correlation indices. That is:

$$\ln SPR = \ln a + bW + cG + dlnRe + \ln LF \ \ldots\ldots\ldots\ldots\ldots\ldots\ldots\ldots\ldots\ldots\ldots\ldots\ldots\ldots\ldots\ldots 4.6$$

But the **observed SPR** is given by equation 4.7

SPR (lb/m) = Sand Concentration (pptb) * Oil Rate (1000 bbl/m)…….…… 4.7

Tables 4.19 and 4.20 show the Reynolds number and SPR data of the investigated well.

Table 4.19: SPR Data determined from Production Data Well G-14

Sand (PPTB)	Oil (bbl/m)	Re	Water (bbl/m)	Water-cut (%)	Gas (Mscf/m)	GLR (scf/bbl)	Observed SPR (lb/m)	Predicted SPR (lb/m)	Deviation (%)
3.00	9188	8.5293E-03	4312.74	31.943	8183.466	606.13	27.6	27.7	0.44
2.00	6400	5.9407E-03	4598.01	41.809	12834.395	1167.00	12.8	13.1	2.05
2.00	3830	3.5556E-03	2946.85	43.482	24331.854	3590.26	7.7	7.7	0.27
7.00	2536	2.3538E-03	1114.55	30.534	37363.758	10235.94	17.7	18.6	4.65
2.00	8500	7.8907E-03	10624.75	55.554	2819.789	147.44	17.0	16.1	5.25
3.00	9952	9.2381E-03	8233.33	45.275	3512.129	193.13	29.9	25.6	14.12
4.00	15200	1.4110E-02	14296.74	48.468	3657.215	123.99	60.8	60.6	0.30
5.00	14062	1.3053E-02	7029.06	33.328	9472.364	449.13	70.3	65.6	6.65
								Average =	4.22

Table 4.20: SPR Data determined from Production Data Well G-15

Sand (PPTB)	Oil (bbl/m)	Re	Water (bbl/m)	Water-cut (%)	Gas (Mscf/m)	GLR (scf/bbl)	Observed SPR (lb/m)	Predicted SPR (lb/m)	Deviation (%)
39.0	14091.040	1.3080E-02	35321.62	71.483	5818.629	117.756	549.6	552.8	0.59
34.0	18137.390	1.6836E-02	13032.26	41.811	83393.244	2675.463	616.7	609.3	1.19
32.0	17323.290	1.6081E-02	12686.08	42.274	2999.026	99.936	554.3	556.1	0.32
32.0	15850.320	1.4713E-02	11520.09	42.090	19275.441	704.244	507.2	480.4	5.29
32.5	19987.840	1.8554E-02	13790.22	40.826	15550.130	460.362	649.6	696.8	7.27
32.5	19149.970	1.7776E-02	13506.97	41.360	16623.504	509.034	622.4	652.9	4.90
34.0	18614.700	1.7279E-02	14326.77	43.492	5912.723	179.492	632.9	636.6	0.59
								Average =	2.88

Using data provided in Tables 4.19 and 4.20, generated linearized systems of equations was solved using MATLAB to determine SPR correlation indices of each well investigated. Summary of the results obtained is presented in Table 4.17.

Table 4.21: SPR Correlation Indices of the Investigated Wells

SPR Correlation Indices				
WELL	a(lb/m)	b	c(bbl/scf)	d
G-14	4.1569E+05	-1.1071	2.45E-04	2.155
G-15	1.7155E+05	1.1633	7.73E-06	1.6751

4.6.6 SPR Model for the Investigated Wells

- For G-14

$$\boldsymbol{SPR} = 415690 * Re^{2.155} * LF * exp(-1.1071w + 2.45E - 04G) \ldots\ldots\ldots\ldots\ldots\ldots 4.15$$

- For G-15

$$SPR = 171555 * Re^{1.16751} * LF * exp(1.1633w + 7.73E - 06G) \ldots\ldots\ldots\ldots\ldots\ldots 4.16$$

4.6.7 Comparison of Predicted SPR based on the model used with Actual SPR of the Wells

Data of predicted SPR and the observed SPR of G-14 and G-15 shown in Table 4.16 and 4.17 respectively will be used to compare predicted SPR and the observed SPR of G-14 and G-15. Figure 4.7 through 4.10 present its graphical for easy visualisation and interpretation.

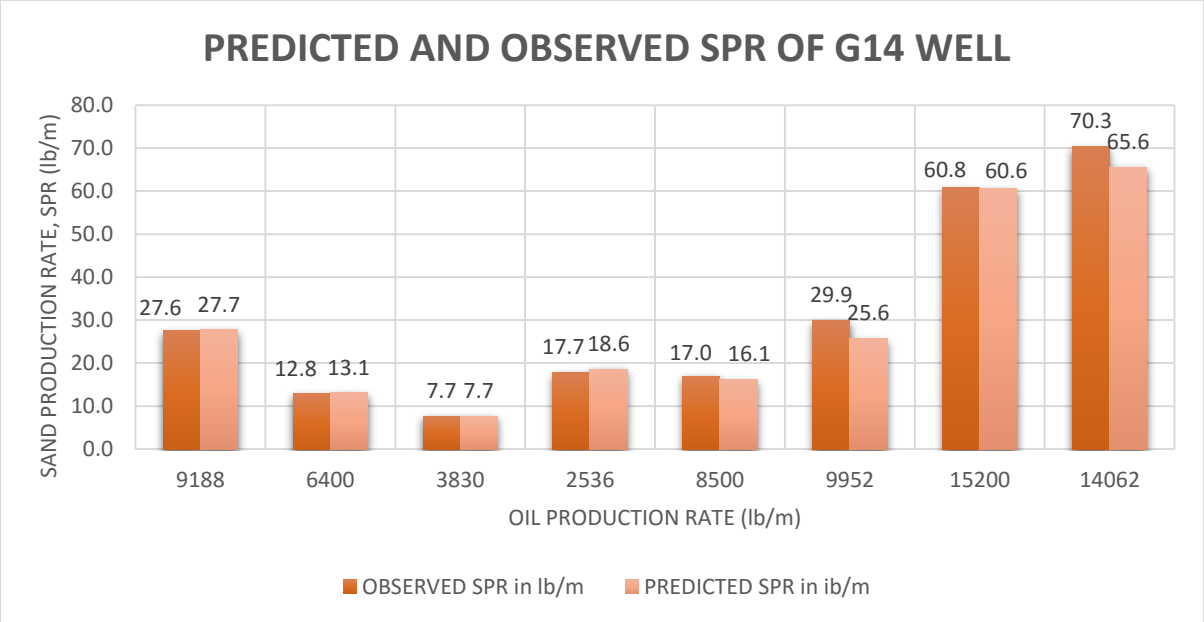

Figure 4.7: Predicted and Observed SPR of G-14 well at different Oil Production Rate

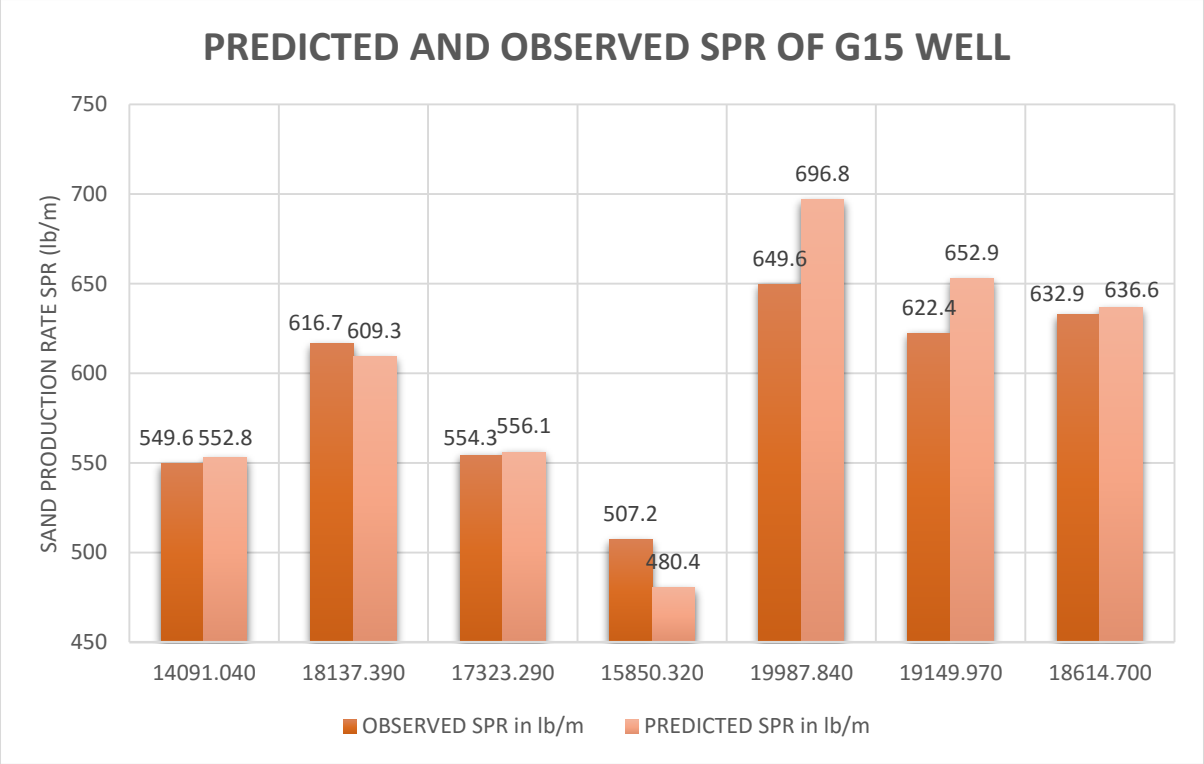

Figure 4.8: Predicted and Observed SPR of G-15 well at different Oil Production Rate.

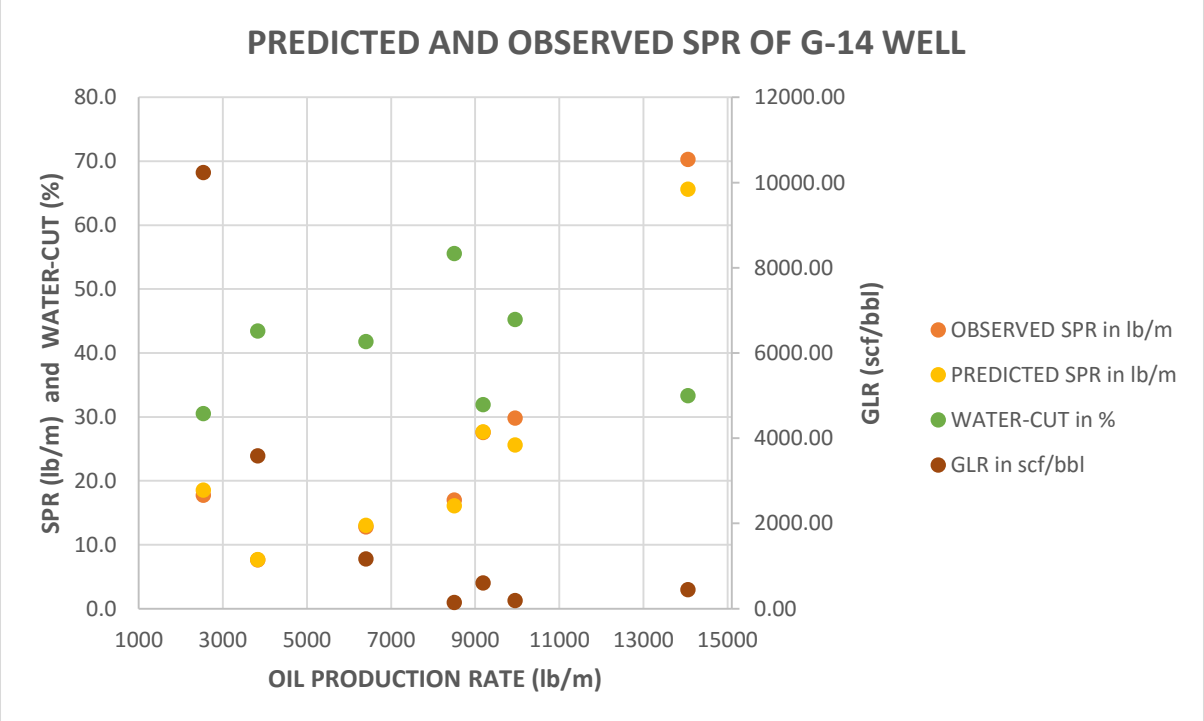

Figure 4.9: Predicted and Observed SPR of G-14 at different Total Liquid Rate

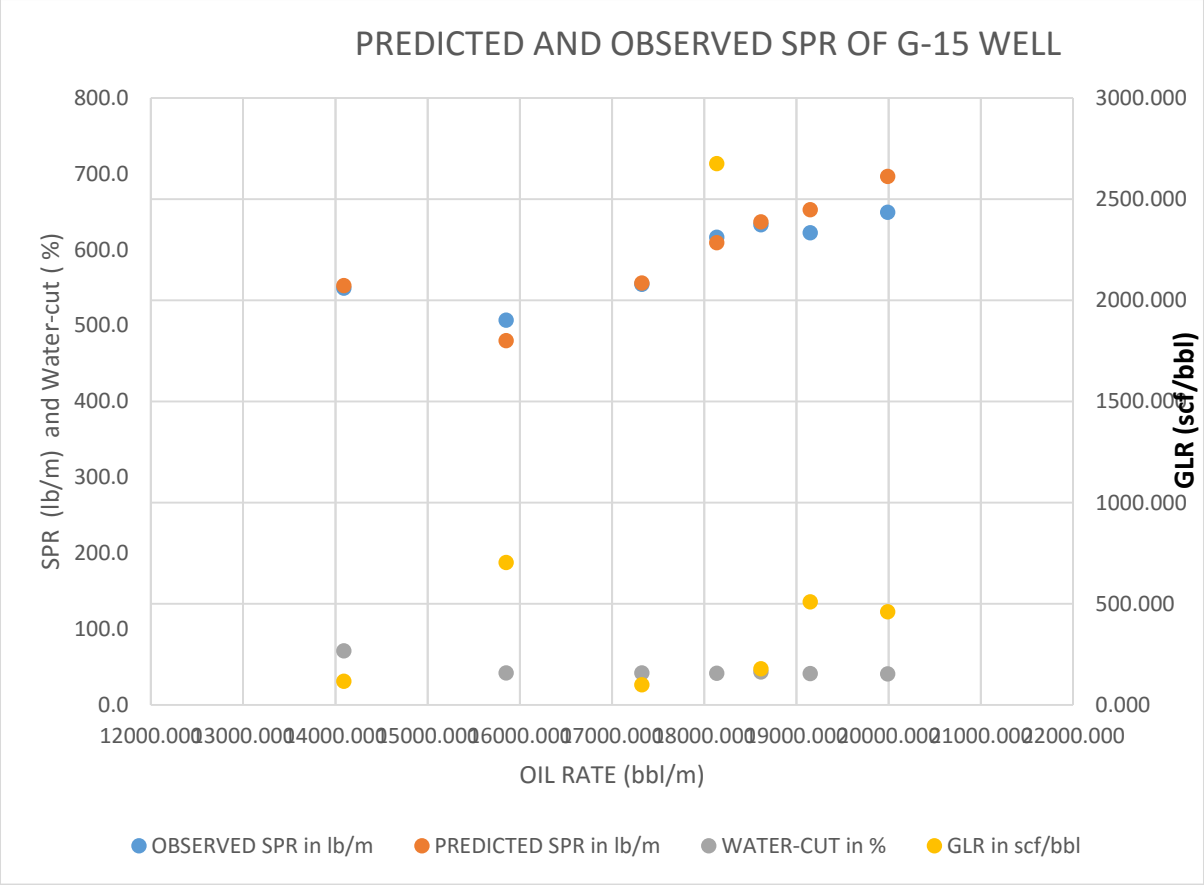

Figure 4.10: Predicted and Observed SPR of G-15 at different Total Liquid Rate

Tables 4.19 and 4.21 show a tabular comparison of predicted SPR and the observed SPR of G-14 and G-15 respectively, while Figure 4.7 through to 4.10 present graphical representations of the predicted and observed model for quick visualisation and interpretation. The model seems to accurately predict quantitatively the rate of sand produced in the investigated wells with an average maximum of 5 % deviation in all case but which is below the tolerance of 10% deviation suggested by the model.

CHAPTER 5

5.0 CONCLUSION AND RECOMMENDATION

5.1 Conclusion

In this work, twenty-two correlations for computing the unconfined compressive strength for rock strength were evaluated for application in the Niger Delta. The best correlation was identified and used to estimate the UCS which was then used to predict the sanding potential of a couple of Niger Delta wells. The three methods used to identify the best correlation for the Niger Delta reservoir are the statistical approach, the rank method and the use of cross plots. From these methods, the Sharma and Singh correlation (correlation 19) was found to be the best correlation. It has the lowest rank of 27.11, the lowest percentage absolute error of 13. 94 and the best cross plot for UCS $\leq$ 75Mpa. This correlation (Sharma and Singh) was applied to predict the critical drawdown pressure (CDP) for sand production favourably with about 7% deviation from measured CDP in some Niger Delta wells.

Using a recent model (Udebhulu and Ogbe, 2015), the results of this study were utilised to predict sand production rate accurately in the investigated Niger Delta wells with an average maximum deviation of 5% in all cases. These results compared favourably to what is expected from the sand production rate predictive model because they fall within the acceptable tolerance of $\pm$10% deviation as suggested by the Udebhulu's model.

The major contribution of this thesis is the identification of the best correlations to estimate UCS in the Niger Delta. UCS is a required input in the prediction of the onset of sand production during oil production, and it is also used in building wellbore stability models often utilized by the oil industry to reduce the cost of drilling and completing wells.

5.2 Recommendations

The following recommendations are suggested to highlight areas of additional research to improve the correlations evaluated in this work.

- Additional dataset from various depositional environments within the Niger Delta should be used to evaluate the UCS correlations.
- Future study should be carried out to use the three best UCS correlations evaluated to build a 3D geomechanical wellbore stability model and compare the result obtained using the three different models to know when each model will fail.

NOMENCLATURE

A	Poroelastic constant
Cs	Cohesion (psi)
C_b	Rock Bulk Compressibility (1/psi)
C_r	Rock Compressibility
CDP	Critical Drawdown Pressure (psi)
E	Young's Modulus (psi)
E_S	Dynamic Shear Elastic Modulus (psi
Ea	Absolute percentage relative error
Er	Average relative percentage error
G	Dynamic Shear Modulus (psi)
GLR	Gas-Liquid ratio (scf/bbl)
ID	Internal Diameter (in)
K	Permeability (mD)
K_b	Bulk Modulus (psi)
LF	Loading factor
n	Number of the perforations
OD	Outside Diameter (in)
P_c	Critical Pressure (psi)
P_R	Average Reservoir Pressure (psi)
P_W	Bottom-Hole Wellbore Flowing Pressure (psi)
TWC	Thick Wall Cylinder Tests

U	Formation Strength (psi)
UCS	Unconfined Compressive Strength (psi)
R	Coefficient of correlation
R_k	Rank
Re	Reynolds's number
S	Standard Deviation
Sa	Absolute Standard Deviation
$S_{i,j}$	Strength of the Statistical Parameter
Sr	Relative standard deviation
SPR	Sand Production Rate (lb/m)
υ	Poisson's Ratio
V_p	P-Wave (Compressional) Velocity (m/s)
V_s	S-Wave (Shear) Velocity (m/s)
Vsh	Shale content (%)
W	Water-cut
X_{log}	Unconfined Compressive Strength from geophysical log (psi)
X_{cal}	Calculated Unconfined Compressive Strength (psi)
ΔP_{de}	Reservoir Pressure Depletion (psi)
ΔP_{dd}	Drawdown Pressure (psi)
ΔP_{td}	Total Drawdown Pressure (psi)
Δt_c	Compressed Sonic Wave Transit Time (μs/ft)
Δt_{ma}	Sonic travel time for matrix mineral grains

Δt_f	Sonic travel time for fluid in the pore space
$\sigma_1, \sigma_2, \sigma_3$	Hydrostatic Stresses (psi/ft)
σ_{twc}	TWC-Collapse Pressure
ρb	Bulk density (g/cc)
β	Non-Darcy flow coefficient
μ	Viscosity (cP)
τ	Shear Strength (psi)
$\emptyset$	Porosity (fraction)
θ	Internal Friction Angle (Degrees)
ε_{ax}	Strain in the axial direction
ε_{lat}	Strain in the lateral direction
σ_n	Stress Normal to the Failure Plane (psi)
σ_1	Overburden stress (psi/ft)
σ_2	Maximum horizontal stress (psi/ft)
σ_3	Minimum horizontal stress (psi/ft)

REFERENCES

1. Adeyanju O.A. and Oyekunle L.O., *''Prediction of Volumetric Sand Production and Stability of Wellbore in a Niger-Delta Formation''* SPE 136965, paper presented at the 34th Annual SPE International Conference and Exhibition held in Tinapa, Calabar, Nigeria, 31 July-7 August, 2010.
2. Adeyanju O.A. and Oyekunle L.O., ''*Experimental Studies of Sand Production from Unconsolidated Sandstone Niger-Delta Petroleum Reservoir'',* SPE 151008, paper presented at the Nigeria Annual International Conference and Exhibition held in Abuja, Nigeria, 30 July- 3 August, 2011.
3. Al-Marhoun, M. A.: "*PVT Correlations for Saudi Crude Oils*," SPE 13718, SPE Middle East Oil TECH CONF and EXHB (Manamah, Bahrain, 11-14 –March 1985).
4. Amaefule J.O., Altunbay M., Tiab, D., Kersey, D.G., and Keelan, D.K.: "Enhanced Reservoir Description: Using Core and Log Data to Identify Hydraulic (Flow) units and predict permeability in uncored Intervals/Wells", paper SPE 26436, presented at the 68th Annual SPE conference and exhibition, Houston, Texas, October 3 - 6, 1993.
5. Chang, C., M. D. Zoback, and A. Khaksar, 2006, ''*Empirical relations between rock strength and physical properties in sedimentary rocks''*: Journal of Petroleum Science and Engineering, 51, 223–237.
6. Djebbar Tiab, *''Rock property and Well log Lecture Note''*: Chapter 1(2B)-Rock properties-porosity and permeability'', AUST 2015.
7. Fidelis Ankwo Abijah and Akaha Celestine Tse, "*Geomechanical Evaluation of an onshore oil field in the Niger Delta"*, 2016.
8. Fjær, E., Holt, R.M., Horsrud, P., & Raaen, A.M. 1992. ''*Petroleum Related Rock Mechanics''*, Development in Petroleum Science, Elsevier, Amsterdam, ISBN 0-444-88913-2.
9. Haimson, B. C. and Fairhurst, C. "*Initiation and Extension of Hydraulic Fractures in Rock''*. SOC. Petrol. Eng., July 1997, pp. 310-318.

10. Mita Sengupta and Keith Katahara," *Linking the Physical and Mechanical Properties of rocks*" DOI http://dx.doi.org/10.1190/segam2012-1129.1, 2012 SEG Annual Meeting in Las Vegas.
11. Musaed N. J. Al-Awad" *Evaluation of Mohr-Coulomb Failure Criterion Using Unconfined Compressive Strength*" King Saud University, College of Engineering, Petroleum and Natural Gas Engineering Department, Riyadh, Saudi Arabia,2012.
12. Nouri, A., Vaziri, H., Belhaj, H. and Islam, R. 2003. "*Comprehensive transient Modeling of Sand Production in Horizontal Wellbores"*. Paper SPE 84500 presented at the SPE Annual Technical Conference and Exhibition, Denver, 5-8 October
13. Ohen Henry A.*" Calibrated Wire line Mechanical Rock Properties Model for Predicting and Preventing Wellbore Collapse and Sanding*" SPE 82236, presentation at the SPE European Formation Damage Conference to be held in The Hague, The Netherlands 13-14 May 2003.
14. Olajide .O. F, and Ikiensikimama, S. S "*Evaluation of Compressibility Factor Correlations for Niger Delta Gas Reservoirs*", Refereed Proceedings, SPE Paper 136967. 34th Annual SPE International Conference and Exhibition held in Tinapa – Calabar, Nigeria, 31 July–7 August.
15. Onuorah, L.O and K. K. Nwozor, "*Optimal Rock Property trends in Normal Pressure Formations in an Offshore Niger Delta Field*', 2014.
16. Sarda, J.-P., Kessler, N., Wicquart, E., Hannaford, K. and Deflandre, J.-P. "*Use of Porosity as a Strength Indicator for Sand Production Evaluation*". Paper SPE 26454 presented at the 68th Annual Technical Conference and Exhibition of the SPE, Houston, TX, 3 -6 Oct. 1993

17. Samuel O. Osisanya, ‘‘*Practical Guidelines for Predicting Sand Production*’’, SPE 136980, paper presented at the 34th Annual SPE International Conference and Exhibition held in Tinapa, Calabar, Nigeria, 31 July-7 August, 2010.
18. Tiab and Donaldson, 2004 “*Petrophysics: the Theory and practice of measuring reservoir rock and fluid transport properties”* Gulf Professional Publishing, USA.
19. Udebhulu, Dickson O. and David O. Ogbe., ‘‘*Mechanistic Model for Predicting Sand Production: a case study of Niger Delta wells’’* SPE 178279- MS, paper presented at the Nigerian Annual International Conference and Exhibition held in Lagos 4-6 August 2015.
20. V. Azizi and H. Memarian,” *Estimation Of Geomechanical Parameters Of Reservoir Rocks Using Conventional Porosity Log’’*, conference Paper School of Mining Engineering, University of Tehran, Iran, 2006.
21. Willson S.M., Moschovidis Z.A., Cameron J.R. and Palmer I.D., ‘‘*New Model for Predicting the Rate of Sand Production’’,* SPE/ISRM 78168, paper presented at the SPE/ISRM Rock Mechanics Conference held in Irving, Texas, 20-23 October, 2002.
22. Woehrl, B., Wessling, S., and Bartetzko, A. and Renner, J.,” *Comparison of Methods to Derive Rock Mechanical Properties from Formation Evaluation Logs*” ARMA 10-167, paper presented at the 44th US Rock Mechanics Symposium and 5th U.S.-Canada Rock Mechanics Symposium, held in Salt Lake City, UT June 27–30, 2010.
23. Zhang, J.J., Rai, C.S., and Sondergeld, C.H**.** “Strength *of Reservoir Materials: Key Information for Sand Prediction.*” SPE Reservoir Evaluation & Engineering 3 (2): 127-131. SPE 62499-PA, 2011.
24. Zoback D, *Reservoir Geomechnics*, published in the United States of America by Cambridge University Press, New York, 2007.